RHODES UNIVERSITY

Where leaders learn

An electrospun nanofiber colorimetric probe for detection of Alkaline Phosphatase for diagnosis of liver toxicity

A thesis submitted in fulfilment of the requirement for the degree of Master of Science in Chemistry

By

Mamello Mohale

Supervisor: Professor Nelson Torto

Acknowledgements

First and foremost, I would like to thank the almighty God for his grace over my life. I am grateful for the precious gift of education he has given me.

I would like to express my sincere gratitude to my supervisor Professor Nelson Torto for his guidance and supervision. I am so overwhelmed by your kindness towards me and the words "THANK YOU" are just not enough. You have believed and invested so much in me and I can honestly say you have steered my academic decisions. Not only have you challenged me to be selfless with my knowledge but to also be open minded and always be willing to help others. I will forever be humbled and honoured to be one of your students.

To Dr. Samuel Chigome, thank you for always encouraging and helping me in any way possible. You have challenged me to become the best researcher I can possibly be and I am forever grateful for your continued support in my academics.

Professor Brett Pletschke and Dr. Susan Van Dyk: It would not be possible to complete this work without the use of equipment in your lab. Thank you for the warm welcome.

Bella, William, Pablo and Joseph: you guys simply just rock our F12 lab. Thank you for always brightening up the lab. Like we always say "F12 for the win, people must know!!!".

To my girls: Tseli, Hafeni, Muthumuni, Moroa, Dineo, Maarasi, and Elaine, you have been true and amazing friends who always encourage me during tough times. I love you guys.

My F12 colleagues: Your constructive analysis of my work has helped me become a better researcher.

Sandisa Imbewu, Research Council, Rhodes University and Chemistry Department: Thank you for funding this work.

I would also like to thank my family for their support more especially my older sister who is one of a kind.

Abstract

A novel electrospun nanofiber colorimetric probe for the detection of Alkaline Phosphatase (ALP) for diagnosis of liver toxicity was developed through electrospinning of a para nitrophenyl phosphate (pNPP) functionalised nylon polymer. The chemical stability of the enzyme substrate (pNPP) and its two products (para nitrophenol (pNP) and para nitrophenolate (pNPL)) was evaluated in biological (pH 7.4), acidic (pH 2) and alkaline (pH 9) pH, respectively. Enzyme kinetics models of Michaelis Menten (MM) and Lineweaver Burk (LB) were used to characterise free ALP. Solution and nanofiber assaying of free ALP and 10x diluted serum (spiked with ALP) was also carried out. The results demonstrated that pNPP and pNP were colourless while pNPL was yellow which indicated that all reagents were chemically stable. In addition, the chromophore of pNPL exhibited a strong molar extinction coefficient (ε) of 18,458 M^{-1} cm^{-1}. LB plot being the most accurate compared to MM showed V_{max}, K_m and excess substrate concentration of 5.5×10^{-3} μmol/min^{-1}, 0.025 mM and 0.25 mM respectively. Solution and nanofiber assaying of free ALP and serum confirmed a direct proportional correlation between the pNPL yellow colour intensity and enzyme activity up to 858 IU/L and 820 IU/L respectively. The dipping of the nanofiber layer into solution showed that the leaching rate of pNPP was extremely high at 1.37×10^{-3} A/min^{-1} as was observed after only the first 0.25 min interval. However, this was not of great concern since it was also observed that administration of the sample (20 μL) by a dropwise method minimised leaching compared to dipping. The preliminary findings on the effect of temperature on the chemical stability of pNPP indicated that it was stable below temperatures of 40 ºC while it hydrolysed at 80 ºC. Therefore a sensitive, rapid and simple colorimetric probe for the detection of ALP was developed. The probe exhibited characteristics that make it suitable to be incorporated into point of care colorimetric liver toxicity diagnostic devices for applications in resource poor settings and telemedicine.

Table of Contents

List of Abbreviations

AIDS	Acquired immunodeficiency syndrome
ALP	Alkaline Phosphatase
AST	Aspartate aminotransferase
AuNPs	Gold nanoparticles
BCIP	5-bromo-4-chloro-3-indolyl phosphate
E.coli	Escherichia coli
EDS	Electron dispersive x-ray spectroscopy
EDTA	Ethylenediaminetetraacetic acid
ELISA	Enzyme linked immunosorbent assay
FDA	Food and Drug Administration
FDP	Fluorescein diphosphate
HaC	Acetic acid
HIV	Human immunodeficiency virus
HPLC	High performance liquid chromatography
IU/L	International Units per Litre
K_m	Substrate concentration at half of V_{max}
LB	Lineweaver Burk
LOD	Limit of detection
ml	Millilitres
MM	Michaelis Menten
nm	Nanometres
OH	Hydroxyl
PDA	Polydiacetylene
pNPP	Para nitrophenyl phosphate
pNP	Para nitrophenol
pNPL	Para nitrophenolate
REDOX	Reduction-oxidation
SEM	Scanning electron microscopy
SPR	Surface plasmon resonance
TEM	Transmission electron microscopy
TN	Tyrosinase enzyme

UV	Ultra violet
Vis	Visible
V_{max}	Enzyme maximum reaction velocity
WHO	World Health Organisation
µg	Microgram
µL	Microlitre
µM	Micromolar
µmol	Micromoles

List of Figures

Introduction

Drug candidates in pre and post clinical stages are the major causes of organ failure with liver toxicity being the most cited reason of concern by the Food and Drug Administration (FDA) [1-2]. Antiretroviral drugs used as therapy for Human immunodeficiency virus infection/acquired immunodeficiency syndrome (HIV/AIDS) have particularly been a notable example of such candidates [3-4]. To date, the World Health Organisation (WHO) estimates that of the 33 million people living with HIV/AIDS worldwide, 68 % of them reside in Sub Saharan Africa [5]. Further, child mortality is estimated to be 90 % due to malaria and HIV/AIDS [6]. Hepatitis B and C co-infections have also emerged as significant contributors to mortality attributed to liver related diseases [5, 6]. Therefore, it is important to continuously monitor the liver's function in HIV/AIDS patients, moreso that 30 % of HIV/AIDS deaths in the developing world are attributed to liver toxicity.

Alkaline Phosphatase (ALP) is one of the biomarkers used in routine clinical diagnosis of liver toxicity [7]. Its function is to catalyse the hydrolysis of a phosphate compound in a variety of tissues (liver, intestine, kidney, and placenta). However, its high levels in blood are indicative of bile ducts failure known as cholestatic liver disease [8-9]. ALP can become markedly elevated approximately ten times the upper limit of normal (≤ 120 IU/L) [10]. The standard method for ALP detection is by colorimetric assaying using a chromogenic substrate of para nitrophenyl phosphate (pNPP). The assay involves hydrolysis of pNPP to a colourless para nitrophenol (pNP) which deprotonates to form a yellow para nitrophenolate (pNPL) compound [11-13]. Enzyme activity is directly proportional to pNPL produced. Although the method is highly sensitive, one of its major shortcomings is not being suitable for point of care applications.

An area where these shortcomings of pNPP assay method has significantly been experienced is in resource poor settings and telemedicine (where distance from health care services is a critical factor). The main challenge has been that the assay method requires instrumentation. In addition, instrumentation is normally expensive and it requires skilled personnel for both operation and maintenance. Furthermore, sample handling time between sample collection points and health care services equipped with appropriate facilities for diagnosis is long [14].

Therefore, there is an urgent need to develop simple, point of care and cost effective probes for vital analytes or biomarkers such as ALP for the diagnosis of liver toxicity.

Electrospun nanofibers have presented themselves as excellent materials for the development of such diagnostic probes. They may act as solid supports for colorimetric indicators [15]. Their unique properties of high surface area to volume ratio, high porosity and ease of functionalisation have also made them highly attractive. In addition, nanofibers are easy to fabricate and there is a wide range of polymers that can be used [16-18]. To the best of our knowledge, no work has been reported on the use of electrospun nanofibers as colorimetric probes for detection of ALP. However in principle, their role as colorimetric probes is similar to that of bioactive paper. For example, Vella and co-workers developed a novel bioactive paper based colorimetric probe for detection of ALP for liver function tests. The paper was used as a solid support for colorimetric substrates of ALP. Diagnosis was based on colour changes associated with the high levels of ALP present in the blood of a patient with liver toxicity [19].

The thesis objective was to design a novel point of care electrospun nanofiber colorimetric probe for detection of ALP for diagnosis of liver toxicity. The nanofibers were used as solid supports to immobilise pNPP. In solution, ALP was characterized using Michaelis Menten and Lineweaver Burk enzyme kinetics models and assayed to determine elevated levels indicative of liver toxicity. Nylon was blended with pNPP and electrospun to synthesise nanofiber composites which were used as colorimetric probes. The thesis is comprised of six chapters. The first chapter discusses the mechanism and diagnostic value of ALP in liver toxicity diagnosis. Chapter two examines the principles of detection techniques for ALP while also establishing their shortcomings from a point of care use perspective. Chapter three presents electrospun nanofibers as suitable point of care colorimetric probes for detection of ALP. Chapter four, five and six outlines the experimental procedure, results and conclusion respectively.

Chapter 1

1. The value of Alkaline Phosphatase biomarker in diagnosis of liver toxicity

Summary

The chapter presents an overview on the mechanism of ALP and its value in routine diagnosis of liver toxicity. Enzyme kinetics models used for its characterisation are also discussed.

1.1 Alkaline Phosphatase

The enzyme of ALP has been one of the most valuable biomarkers used for diagnosis of cholestatic liver disease [20]. Elevated levels in the blood are indicative of total bilirubin dysfunction which is related to liver damage. Cholestasis is a manifestation of defective bilirubin responsible for secretion of bile and urine [21-22]. During the process of cholestasis, there is a high accumulation of cytotoxic bile acids which eventually affects the liver. In order for the liver to counteract this process, nuclear receptors regulated pathways will try to coordinate bile acids and secretion homeostasis to minimise the detrimental effects. However, continued exposure of bilirubin to defective inducers such as HIV/AIDS drugs, alcohol abuse, genetic disorder and legion of biliary tract can ultimately cause severe liver damage [23]. As a result, the levels of ALP can rise significantly even up to ten times the upper limit of normal (≤120 IU/L) [24]. For this reason, it has become highly critical to monitor the enzyme activity (IU) of ALP. Activity can be accurately determined by understanding the enzyme kinetics and mechanism action of ALP.

In clinical diagnosis, the levels of ALP enzyme activity are commonly determined by the use of continuous and discontinuous assay methods [25]. In the former, activity is measured in real time while in the latter, the reaction is stopped and then samples are taken afterwards. Each method has its advantages and drawbacks. For continuous assay, the advantage is that the initial rate of ALP can be monitored with confidence while the drawback is that only one measurement can be taken at a time. In discontinuous assay, the advantage is that readings can be taken in unit time which means it is highly time efficient. It also has a better sensitivity compared to its counterpart. The disadvantage is that partial stopping of the reaction can give rise to errors [26-27]. However, discontinuous assay has gained more popularity amongst clinicians because of its advantages. Moreover, elucidation of the active site also revealed that

it is much easier and quicker to stop the reaction using competitive inhibitors. Therefore, understanding the mechanism of the active site is important to design accurate assay methods.

The three dimensional structure of ALP reveals that it is a dimer with two identical subunits each comprising of 449 amino acid residues. Its molecular weight ranges between 80,000 and 89,000 [28-29]. The role of ALP is to hydrolyse a phosphate monoester bond by formation of a phosphoseryl intermediate which dissociates to form a free phosphate and an alcohol as products (Fig. 1.1) [30]. Its mechanism of action in the active site is illustrated schematically in Fig. 1.2. There are two Zn^{2+} and one Mg^{2+} metals cofactors which have a responsibility of binding the substrate. Hydrolysis occurs by a nucleophilic elimination. Firstly, the phosphoserly group coordinates to the two zinc metals. Secondly, there is an attack on the phosphoserly by serine (ser 102) residue nucleophile. Lastly, the intermediate dissociates with the release of a phosphate as the leaving group. Hydroxides bound to Mg^{2+} act as bases that deprotonates the serine nucleophile to attack the phosphoserly [31-33].

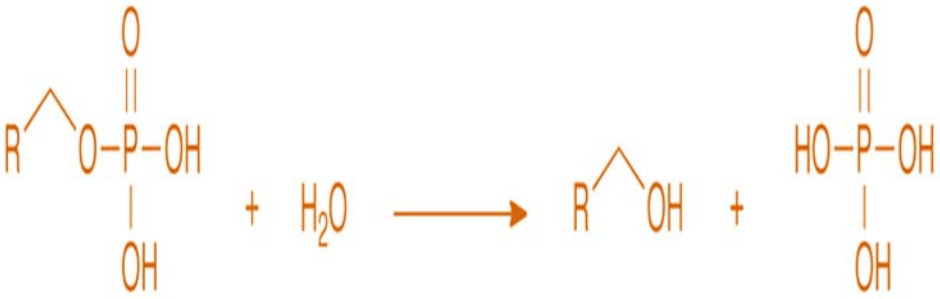

Phosphate monoester bond Alcohol Phosphate

Figure 1.1: Catalytic mechanism of ALP. A phosphate monoester bond is hydrolysed by ALP to form an alcohol and a free phosphate as products.

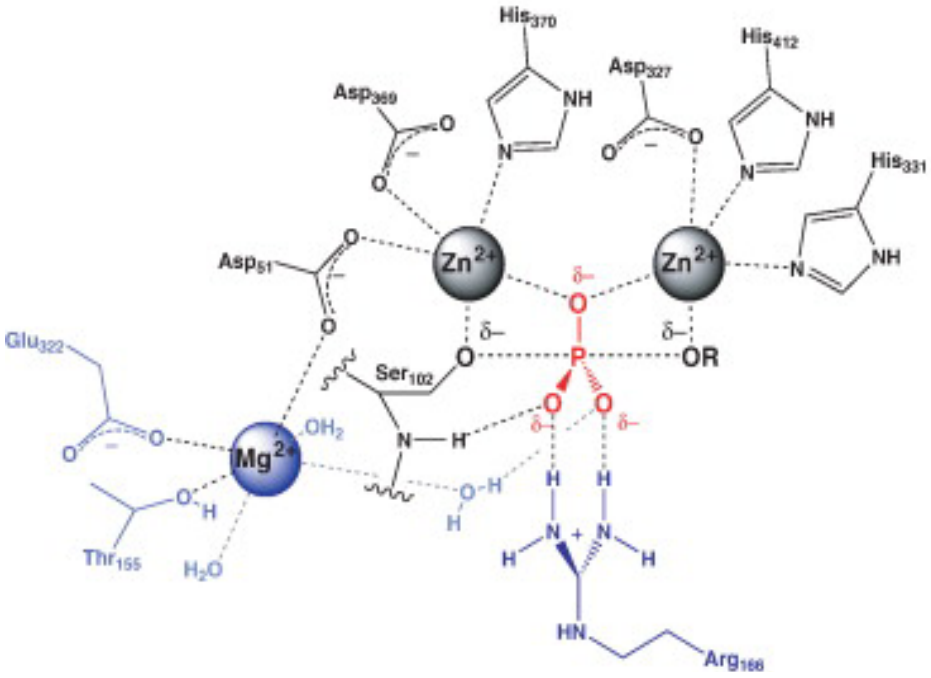

Figure 1.2: Active site of ALP from *E.coli*. There are two Zn^{2+} and Mg^{2+} cofactors metals present in the active site to coordinate the substrate [33].

Elucidation of the active site has been useful in identifying ethylenediaminetetraacetic acid (EDTA) as the most effective competitive inhibitor that could be used for discontinuous assays [34]. EDTA is a strong chelator of metals that can inactivate ALP by binding the Zn^{2+} and Mg^{2+} metals. Further, understanding the active site has also been beneficial in determining the appropriate sample matrix that could be used to achieve accurate measurements. For instance, serum has been identified as the suitable sample for assaying because plasma contains anticoagulants (such as EDTA and heparin) which inhibit ALP [35]. Finally, the most important aspect of studying the active site has been in characterisation of ALP using enzyme kinetics models. The models can indicate the interactions of ALP with its substrate in the active site and have thus also become necessary to study.

Michaelis Menten (MM) is the most commonly used enzyme kinetics model for ALP. The important kinetics parameters monitored are V_{max} (maximium reaction velocity), K_m (substrate concentration at half of V_{max}) and K_m/V_{max} (catalytic efficiency) [36-37]. MM (Fig. 1.3) is expressed in terms of enzyme substrate concentration versus the rate of reaction which can increase in an asymptotic fashion with increase in substrate concentration as it approaches V_{max} [38-39]. Half of V_{max} is the K_m value which can also be observed in Fig. 1.3. At high substrate concentrations, the active sites become saturated and the rate of the reaction reaches

a plateau as there are no available sites to bind the excess substrate. Although MM has been highly popular, it is susceptible to errors due to the difficulty in experimentally measuring the initial rate of reaction and so clinicians prefer to employ Lineweaver Burk (Fig. 1.4) to linearise the data [40-41]. The linearised plot is based on double reciprocal of MM and is advantageous in that it gives greater emphasis on points at low substrate concentration that are subject to experimental error. Alternative plots that can also be used for linearising the data are Hanes and Eadie-Hofstee.

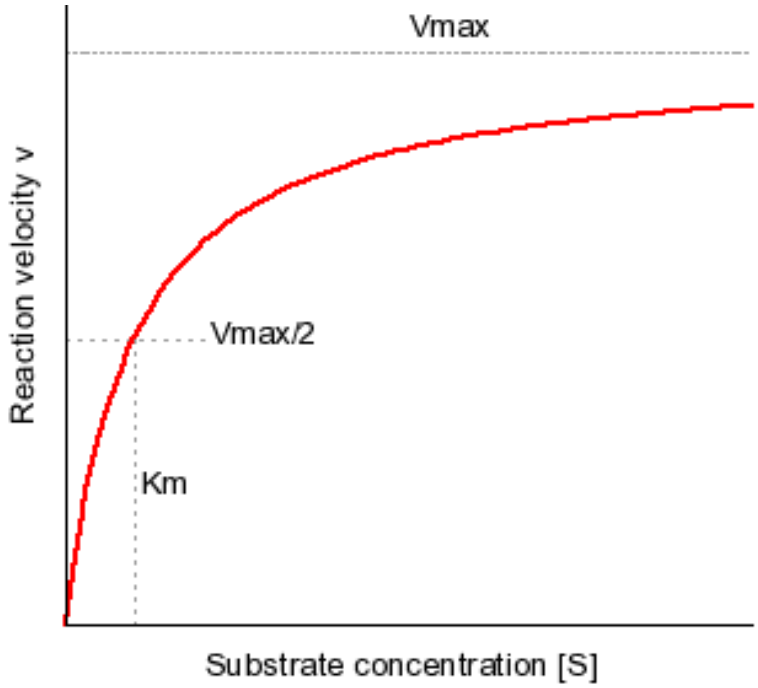

Figure 1.3: Michaelis Menten curve. The rate of the reaction increases asymptotically with increase in the substrate until a plateau is reached [42].

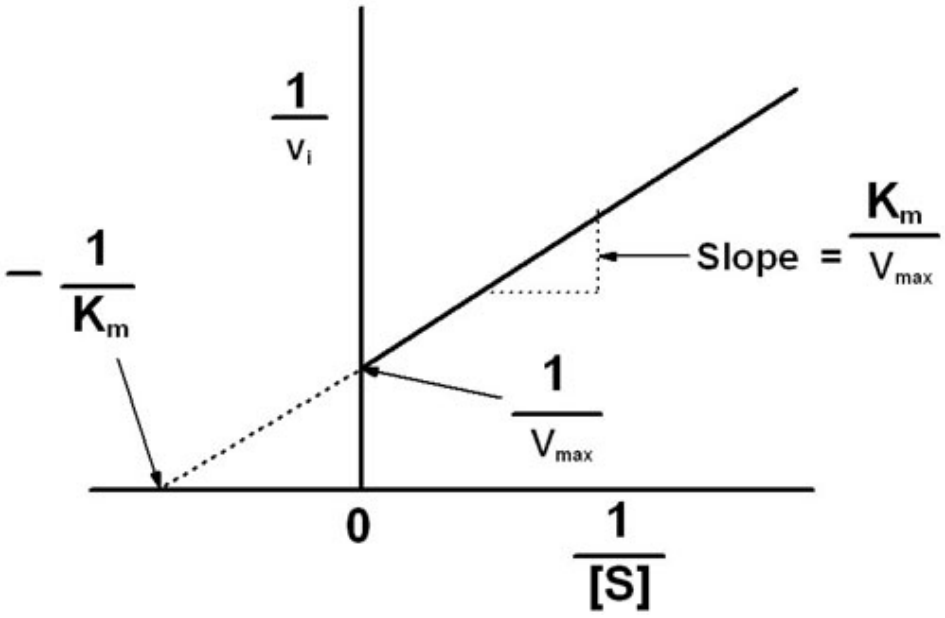

Figure 1.4: Lineweaver Burk plot. The plot is a double reciprocal of the linear portion of Michaelis Menten curve [43].

One of the major applications of the models has been in elucidation of the effects of concentration, inhibitors, pH and temperature on the enzyme activity of ALP [44]. The models have also been valuable in the design of synthetic substrates for colorimetric assaying of ALP. For example, a substrate with a higher K_m would indicate low affinity to ALP and would therefore not be suitable for assaying [45].

Therefore ALP is highly valuable in diagnosis of liver toxicity induced by cholestasis. Elucidation of the active site and mechanism of ALP is important in developing better assay methods. Enzyme kinetics are useful tools for characterisation of ALP. Therefore, the next chapter will present conventional techniques employed for the detection of ALP in diagnosis of liver toxicity.

Chapter 2

2. The principles of detection techniques for Alkaline Phosphatase

Summary

The chapter will discuss the principles behind the techniques used in detection of ALP for diagnosis of liver toxicity. The chapter presents their advantages but also addresses some of their drawbacks in relation to diagnosis in resource poor areas where telemedicine is practiced. The discussion is limited to the following techniques; chromogenic substrate, surface plasmon resonance, fluorescence, chemiluminescence, electrochemical and immunochemical based detection.

2.1 Detection techniques for Alkaline Phosphatase.

Diagnosis of cholestatic liver toxicity does not only rely on understanding the mechanisms of ALP as discussed in the previous chapter, but also on the ability to accurately detect the enzyme. There are several techniques conventionally employed as most have the attractive features of high sensitivity and selectivity. However, since they require instrumentation, they have been proven not to be suitable for point of care applications in resource poor areas. Some of the main reasons have been that expensive instrumentation, sample preparation and skilled personnel are required for their operation. As a result, the wellbeing of patients with liver toxicity in these areas has usually been compromised due to the fact that feedback is not immediate. These challenges have thus encouraged researchers to develop portable, cost effective and sensitive self-integrated devices suitable for diagnosis.

Lab on a chip colorimetric probes for detection of ALP are a classic example of such devices since they are able to carry out the diagnosis procedure without the use of heavy instrumentation. However, because their detection principles are similar to those of conventional techniques, it is important to establish the drawbacks that present these techniques as not being appropriate for point of care applications in resource poor settings. Further, it is also important to address their advantages from a diagnosis point of view in terms of their sensitivity and ability to detect ALP. Therefore chromogenic substrate, surface plasmon resonance, fluorescence, chemiluminescence, electrochemical and immunochemical based detection techniques for ALP will be reviewed.

2.2 Chromogenic substrate based detection

Detection of ALP based on the use of chromogenic substrates is a widely utilised technique in routine diagnosis for liver toxicity. The technique has gained popularity due to the fact that quantification is easy as it relies on the formation of colours. There are many substrates currently available in the market but the standard one is para nitrophenyl phosphate (pNPP). It is a phenolic compound with a nitro and a phosphoseryl group attached to the para positions of the benzene ring. [46]. The procedure for detection involves hydrolysis of pNPP by the enzyme (Fig. 2.1). Then a colourless para nitrophenol (pNP) is produced which deprotonates to form a yellow colour of para nitrophenolate (pNPL). Increase in the colour intensity can be measured by a spectrophotometer at a wavelength of 405 nm since the intensity translates directly to the enzyme activity of ALP. The product of pNPL has a molar extinction coefficient (ε) of 18, 400 M^{-1} cm^{-1} which means the chromophore can strongly absorb in the visible region of the electromagnetic spectrum [47]. The yellow colour is a result of π electrons resonance shift which causes the molecule to strongly absorb the visible light [48-49].

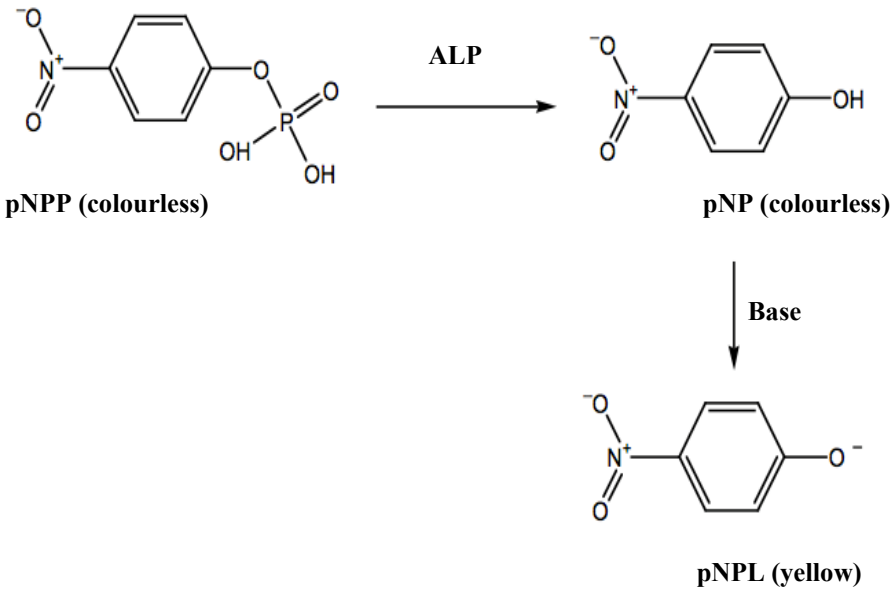

Figure 2.1: pNPP mechanism of detecting ALP. Chromogenic substrate of pNPP is hydrolysed by ALP to pNP and both are colourless. Deprotonation of pNP to pNPL in basic conditions induces a yellow colour which is directly proportional to the enzyme activity of ALP.

The advantage of chromogenic substrate based assay is that analysis is quick (assay can be carried out in less than 1h) even under non-standard conditions. It is also highly selective due to good enzyme-substrate affinity while the strong chromophore of pNPL also makes taking readings easy [50-52]. On the other hand, the main disadvantage is that a spectrophotometer is required which can be expensive. Further, it requires skilled personnel who can operate the instrumentation and also carry out sample preparation [53]. Sample holders such as cuvettes and microtitre plates can also add to the cost of the instrument. These drawbacks have therefore presented chromogenic based substrate method as not being appropriate for point of care use.

2.3 Localized surface plasmon resonance detection

Advances in nanotechnology have shown gold nanoparticles (AuNPs) to be better alternative colorimetric moieties over traditional chromophores such as pNPP. Their extremely higher extinction coefficient has been a major reason for the shift in using them to detect ALP. Furthermore, AuNPs are highly selective because they can easily be functionalised with substrates recognisable to ALP [54-56]. Detection is also quick because hydrolysis of the phosphate ester can induce colour changes whose intensities are directly proportional to ALP. AuNPs are also highly optical due to localized surface plasmon resonance (LSPR) induced by a collective oscillation of surface electrons upon electromagnetic radiation in the visible region of the electromagnetic spectrum [57].

The general principle of detection is based on colour changes attributed to the ability of the AuNPs to disperse or aggregate. Dispersed AuNPs have a LSPR absorption band in the blue region on the electromagnetic spectrum and therefore appear red. Conversely, aggregated AuNPs absorb in the red region of the spectrum which results in their blue colour [58-60]. Agglomeration is due to the London van der Waals forces between the gold atoms. Therefore, substrate ligands that can counteract these forces and selectively recognise ALP are commonly used. Colour changes are induced by hydrolysis of the substrates by ALP.

A notable example of application of AuNPs to detect ALP was reported by Choi and co-workers [61]. Their rational was that if the AuNPs were functionalised by ALP substrate (H2N-Cys-Try (PO32-)-Arg-OH), the nanoparticles would be dispersed and thus exhibit a red colour (Fig. 2.2). Once the phosphate group was hydrolysed, peptide induced aggregation

would be triggered resulting in a blue colour. The colour changes would be monitored by a spectrophotometer while the nanoparticles would be visualised using transmission electron microscopy (TEM). Possible interactions hypothesised between ALP and the AuNPs were hydrophobic, hydrophilic, π-π stacking, electrostatic and steric [62].

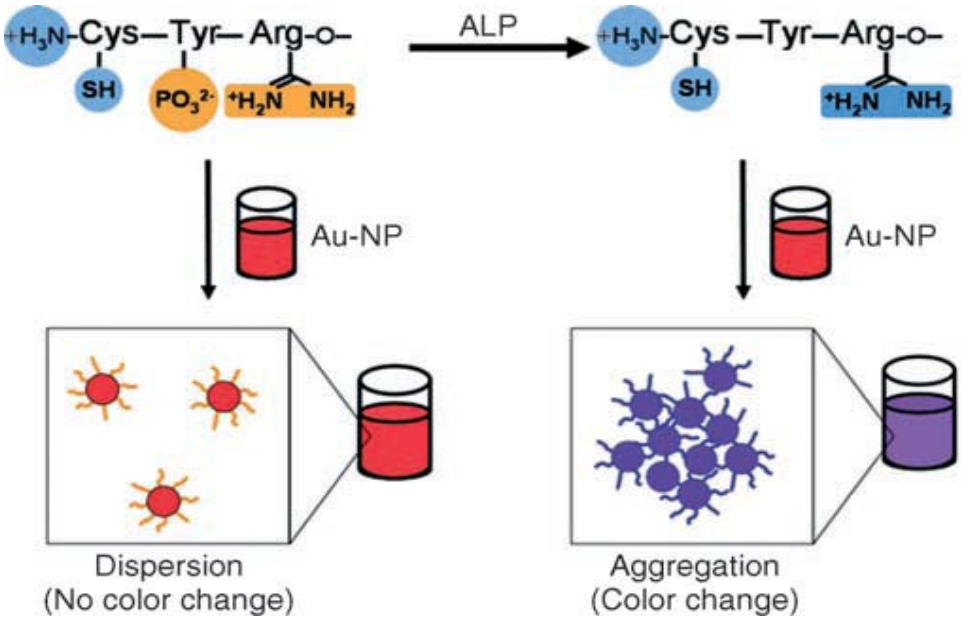

Figure 2.2: Alkaline Phosphatase assay based on colour changes during peptide AuNPs aggregation. The AuNPs substrate is red and turns blue upon hydrolysis by ALP [61].

The surface plasmon resonance technique also suffers from similar disadvantages as chromogenic substrate based in that both require instrumentation. Reproducibility of AuNPs synthesis can also be another drawback experienced with surface plasmon resonance based detection technique.

2.4 Fluorescence detection

Fluorescence is described as the emission of light by molecules that have absorbed photons. As can be deduced from the Jablonski plot (Fig. 2.3), the incident laser beam firstly strikes the molecules with photons. Secondly, the molecules absorb energy which excites them from ground state (S_0) to excited higher energy state (S_1) [63]. Thirdly, there is a relaxation of the

molecules first to the lowest energy of the excited state (rate of femseconds to picoseconds) which results in stokes shift. The stokes shift describes that fluorescence photons have longer wavelengths than absorption photons [64]. Moreover, lifetime of molecules (nanoseconds) before rapid decay to the ground state of lower energy (S_0) can occur and it is this process referred to as fluorescence.

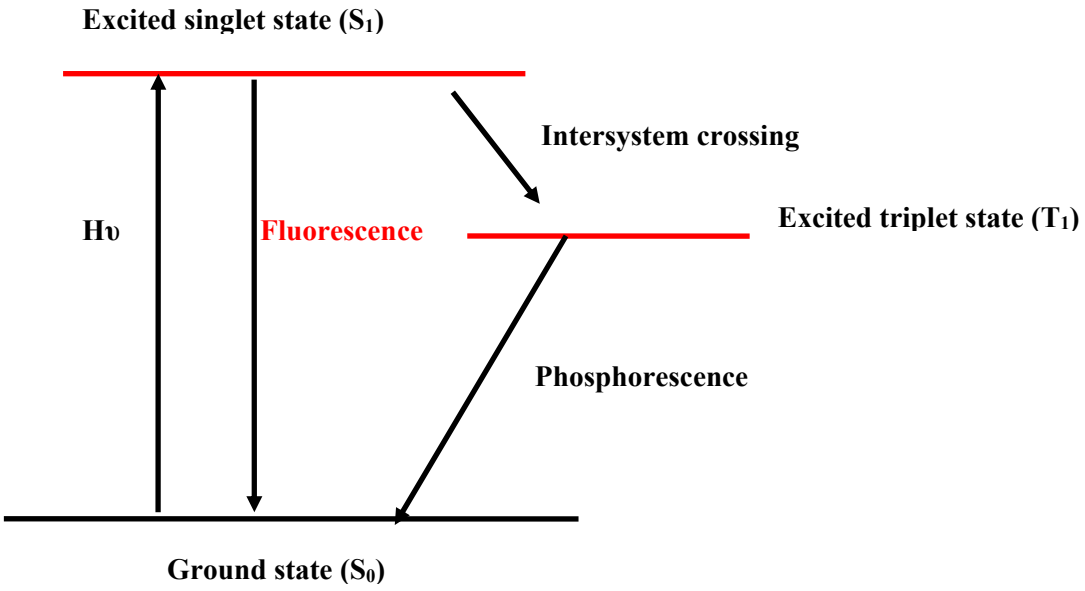

Figure 2.3: Jablonski diagram. Fluorescence occurs when the molecules relax from excited singlet state (S_1) to the ground state (S_0).

In the detection of ALP, the most sensitive fluorephore that has commonly been used is fluorescein diphosphate salt (FDP) (Fig. 2.4). It is a highly conjugated molecule derived from phthalicandydride and two resorcinol groups using zinc chloride as a catalyst via Friedel Craft reaction [65]. The two resorcinol groups are functionalised with two phosphate groups which can be hydrolysed by ALP. FDP is initially non fluorescent and colourless but upon hydrolysis of the phosphate groups, it becomes highly fluorescent and produces a green colour. The first step involves removal of the first phosphate followed by removal of the second one after which a deep green fluorescence colour is formed. Enzyme activity is monitored by increase in the colour intensity. Maximum absorbance is at 494 nm while emission is at 521 nm [66-68].

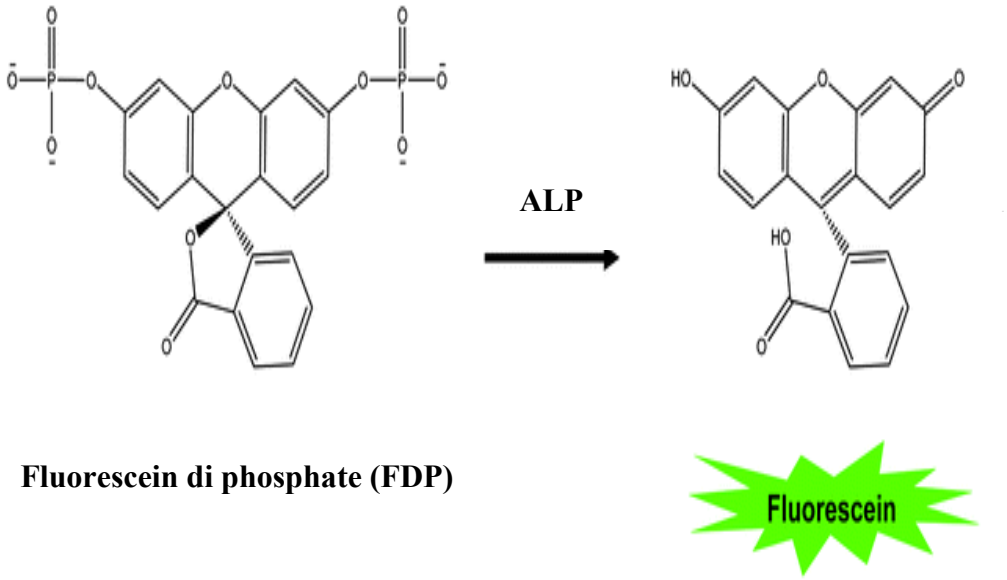

Figure 2.4: Fluorescence detection of ALP using fluorescein di phosphate substrate. Hydrolysis of the substrate by ALP results in formation of a fluorescein moiety [69].

There are many advantages of the fluorescence method in relation to diagnosis of liver toxicity. It is highly sensitive (up to 50 times more than pNPP chromogenic substrate based methods) due to the specificity of the fluorescein to ALP. The fluorescein has a higher molar extinction coefficient (ε) of 90, 000 M^{-1} cm^{-1} which makes taking readings easy. It also has a stronger quantum yield above 0.90 which also enhances sensitivity [69-70]. High assay pH of 7.4-8 also increases fluorescence significantly.

Fluorescence method however suffers from complex data interpretation because of the formation of two products; the fluorescein monophosphate (has minimum fluorescence) and the fully hydrolysed fluorescein (has maximum fluorescence) [69]. If the former is more abundant, then misdiagnosis can occur as it is highly essential for the two phosphates to be totally removed. As with any spectrometric technique, the method relies heavily on instrumentation (fluoremeter) meaning quantification of enzyme activity cannot be carried out in its absence. Further, the complexity of data interpretation means unskilled personnel cannot deduce the implications of the data.

2.5 Chemiluminescence detection

Chemiluminescence is observed when excited states are derived from products of a chemical reaction rather than from absorption as is the case in fluorescence. Nonetheless, the fundamental principles between the two are the same as chemiluminescence is associated with emission of light [71]. A luminophore is excited to a higher energy level and upon relaxation, luminescence emission light is produced. For detection of ALP, a luminophore substrate of 1.2 dioxetane modified with a phosphate is commonly used (Fig. 2.5). In principle, the four membered dioxetane ring acts as the source of energy for the reaction while the adamantly group is responsible for stabilising the ring [72-74]. During the chemical reaction, ALP hydrolyses the phosphate ester bond on the dioxetane which results in the production of a phenoxide intermediate. Then the unstable intermediate decomposes with the emission of prolonged glowing light (475 nm) which is a direct measure of activity [75].

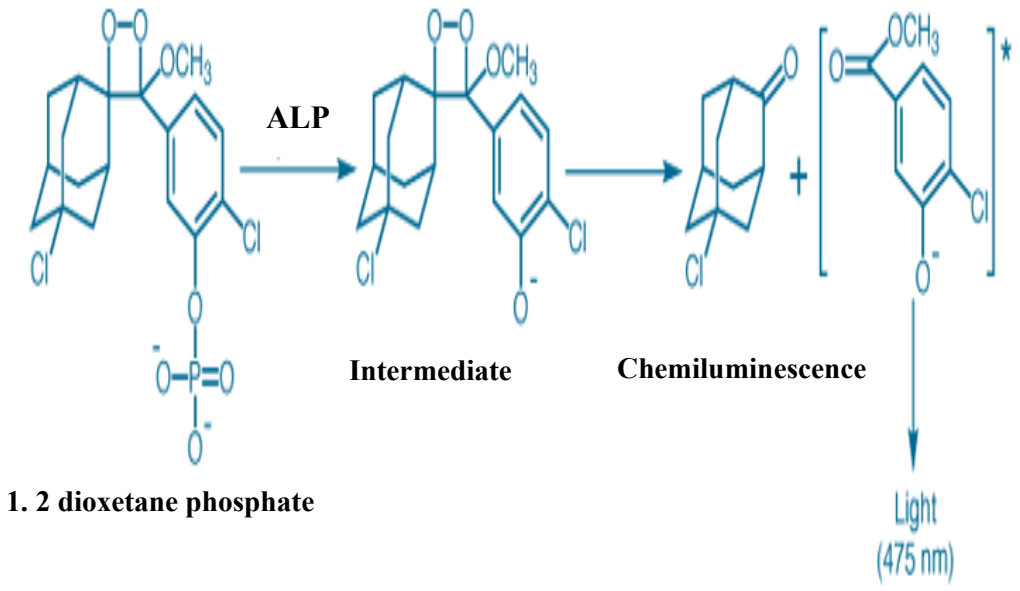

Figure 2.5: Chemiluminescence detection of ALP using 1.2 dioxetane phosphate substrate. The substrate is hydrolysed by ALP and decomposition of the intermediate results in chemiluminescence [76].

The attractive features of chemiluminescence are the high stability of substrates at room temperature and the rapid analysis time (less than 10 sec). It is also highly sensitive. However, despite these advantages, chemiluminescence remains by far one of the most expensive detection techniques due to the expensive nature of the luminometer instrumentation [77-78].

Substrates also tend to be expensive because of the complexity involved in synthesising them. As a result, chemiluminescence method has not gained much popularity amongst clinicians in general.

2.6 Electrochemical detection

Clinical diagnosis of liver toxicity has seen a growth in the use of electrochemistry techniques for assaying of ALP over the years. Electrochemistry is concerned with transfer of electrons in solution at the interface of an electrode and electrolytes using potential to drive the reaction [79-82]. There are several modes employed for detection of species produced during electrochemical reactions but amperometry has been the most common for assaying of ALP [83-84].

In amperometry mode, substrate phenyl phosphate structurally similar to pNPP is used and when ALP hydrolyses the phosphate ester bond under alkaline condition (pH 10), a phenol is produced (Fig. 2.6). The second step involves a tyrosinase enzyme (TN) which oxygenates the phenol to a catechol under acidic conditions (pH 6.5) on a carbon paste electrode. Catechol is oxidised to an o-quinone molecule in a reversible manner and an amperometer is used to measure the redox reaction. Production of the phenol is monitored by determining the current from reduction of o-quinone by catechol mediator (donates two electrons) [85-86]. The current is directly proportional to the concentration of phenol produced which is also proportional to ALP activity. Phenol oxygenase can also be used as an alternative for oxygenation of the phenol group to catechol.

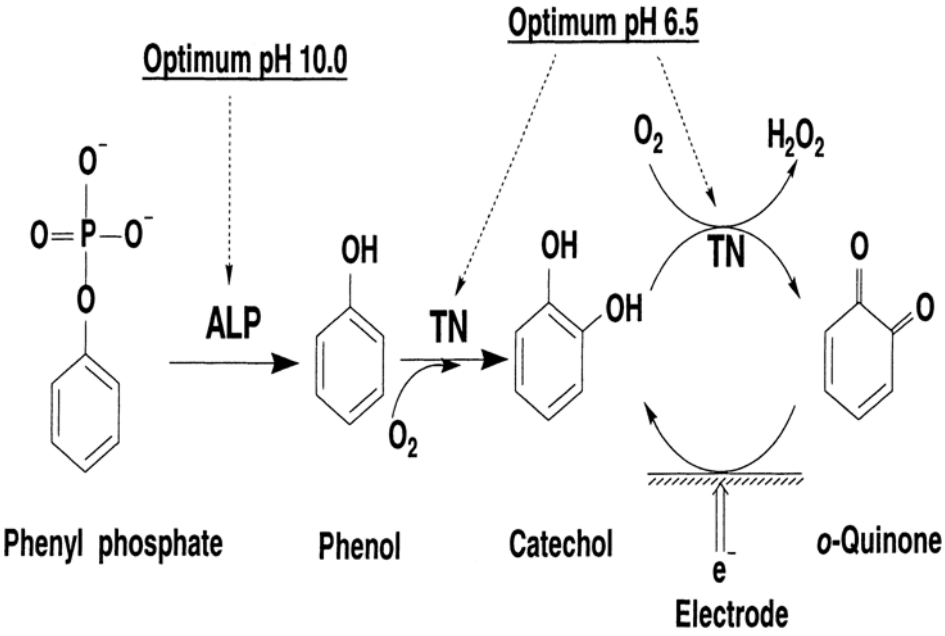

Figure 2.6: Electrochemical detection of ALP by amperiometric mode. Phenyl phosphate is hydrolysed by ALP under basic conditions and a phenol is produced. Tyrosinase (TN) enzyme is used to oxygenate the phenol to catechol. Enzyme activity of ALP is measured by monitoring current produced during oxidation of o-quinone by the catechol [85].

The electrochemical detection technique has the advantages of being highly selective through the use of REDOX potential, versatile, amenable to automation and cost effective [87]. On the contrary, the disadvantages are that multiple enzyme reactions can be tedious and small electrode surface can limit efficient mass transport [88]. Further, the electrode is not durable as it can easily wear off due to mishandling and use of corrosive solvents. Therefore these drawbacks tend to present electrochemical detection as not being suitable for applications in resource poor settings.

2.7 Immunochemical detection

Immunoassay technique has gained popularity in diagnosis of liver toxicity since its development in 1960 by Yalow and Berson. It is based on the specific interactions between an antigen and an antibody [89-90]. Immunoassay can either be heterogeneous (reaction takes place on a solid support) or homogeneous (reaction takes place in solution) but the former is normally preferred since it is much easier to construct [91-93]. Enzyme linked immunosorbent assay (ELISA) is the most widely used form of immunoassay and there are three different types which are direct, indirect and sandwich. However, for detection of ALP, sandwich is commonly employed.

In sandwich based ELISA, the three antibodies involved are capture, detecting and secondary. ALP is attached to the secondary while the antigen is sandwiched between the capture and detecting antibodies (Fig. 2.7). The chromogenic substrate of choice is usually 5-bromo-4-chloro-3-indolyl phosphate (BCIP) which is hydrolysed to 5-bromo-4-chloro-3-indole intermediates [94-95]. Detection is based on coupling of the intermediates since they produce an indigo colour which is directly proportional to the enzyme activity of ALP. Unbound antibody sites should also be blocked using proteins such as bovine serum albumin to prevent nonspecific binding of the enzyme as sensitivity may be reduced.

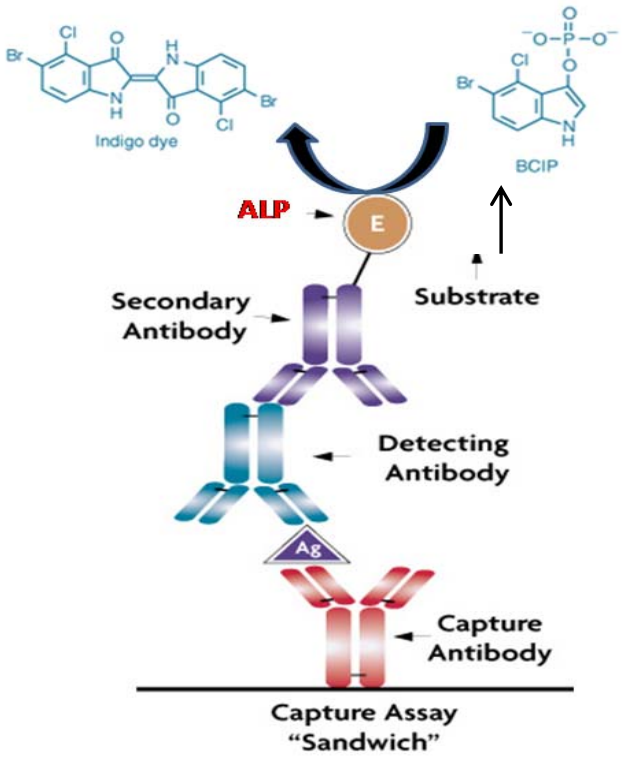

Figure 2.7: Sandwich immunoassay detection of ALP. There are three antibodies used which are capture, detecting and secondary. ALP is covalently attached to the secondary antibody and 5-bromo-4-chloro-3-indolyl phosphate is the commonly used substrate. Hydrolysis of the substrates results in an indigo colour that is directly proportional to the activity of ALP [96].

Sandwich assay has the advantage of being highly sensitive due to amplification of the signal by the three antibodies. Complex matrices such as blood can also be easily analysed since sample preparation is not necessary [97]. The method is also highly versatile because there are a large number of experiments that can be carried out using the same primary antibody. As

with chemiluminescence, ELISA remains one of the most expensive techniques due to the multiple steps involved in its construction.

To conclude, fluorescence, chemiluminescence, electrochemical and immunochemical are the most sensitive techniques for the detection of ALP compared to chromogenic substrates and surface plasmon resonance based techniques. However, chemiluminescence and immunochemical remain by the far the most expensive techniques. Further, all the techniques are not suitable for point of care applications since they require expensive instrumentation and skilled personnel. Therefore, the next chapter will present electrospun nanofibers as better alternatives to these conventional techniques for point of care diagnosis of liver toxicity.

Chapter 3

3. Electrospun nanofiber colorimetric probes for detection of Alkaline Phosphatase

Summary

The chapter presents a review on electrospun nanofibers as solid supports for the design of a colorimetric probe capable of detecting ALP for point of care diagnosis of liver toxicity.

3.1 Electrospun nanofibers as solid supports for colorimetric probes

Nanomaterials of electrospun nanofibers have been used as solid supports in colorimetric probes to immobilise substrates capable of enzyme recognition. Electrospun nanofibers have a unique property of large surface area to volume ratio which allows for maximum interactions between the substrate and the enzyme. Their ease of functionalisation with substrates and high porosity has also made them highly attractive as solid supports [16-18]. Mass transfer is also highly efficient due to the open framework of the nanofiber. Further, the facile process of electrospinning has presented electrospun nanofibers as suitable solid supports because of ease of fabrication. There is a wide range of both natural and synthetic polymers that can be used to synthesise them. Immobilisation of the substrates is also easy since it can be achieved by non-covalent or covalent bonding even though the latter is commonly preferred to prevent leaching [98]. These unique properties have therefore been the basis upon which nanofibers are considered to be suitable solid supports for colorimetric probes.

3.2 Electrospinning

The process of electrospinning relies on repulsive forces to draw a viscoelastic solution such as a polymer into nanofibers [99-100]. Electrospinning can either be nozzle or nozzleless based however the former will be discussed since it is much easier and less expensive to set up. Components that fulfil the nozzle electrospinning process are a high voltage supplier, a capillary tube with a small diameter needle and a collector plate (metal) (Fig. 3.1). During electrospinning, voltage is applied to the needle tip and a spherical taylor cone (Fig. 3.2) is formed by the viscoelastic solution due to accumulation of surface charge. As voltage is increased to overcome the surface charge, a jet is ejected from the apex of the taylor cone. Then surface tension built up by the charges creates a bending motion of the jet [101-105]. The voltage eventually overcomes the surface tension and it is during this stage that the

viscoelastic solution jet stretches to form nanofibers which are deposited on the grounded collector.

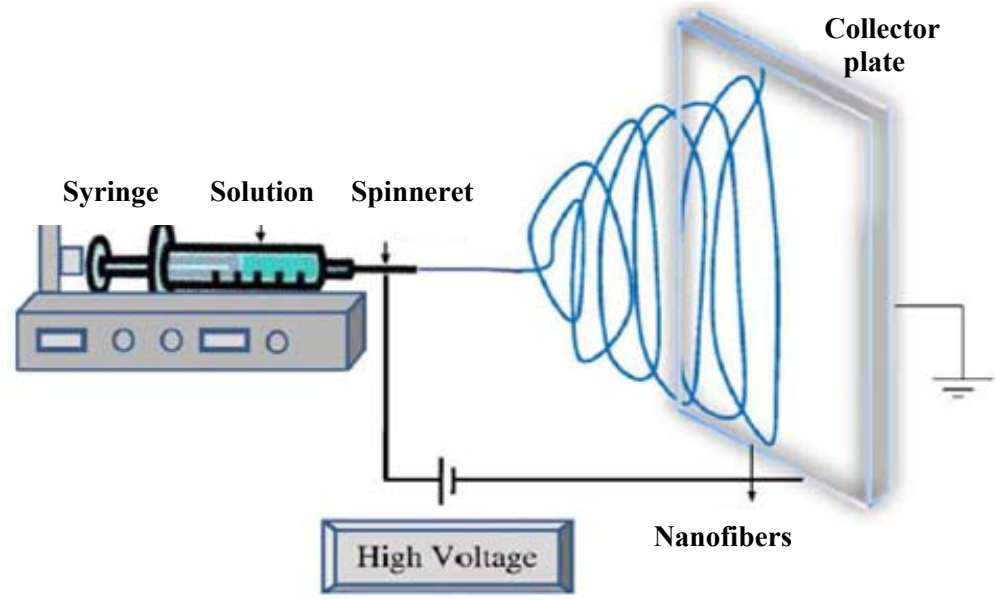

Figure 3.1: Basic components of nozzle based electrospinning. A syringe with a viscoelastic solution is mounted onto a dispenser and when voltage overcomes the surface tension on the spinneret, the solution is drawn into nanofibers deposited on the collector [106].

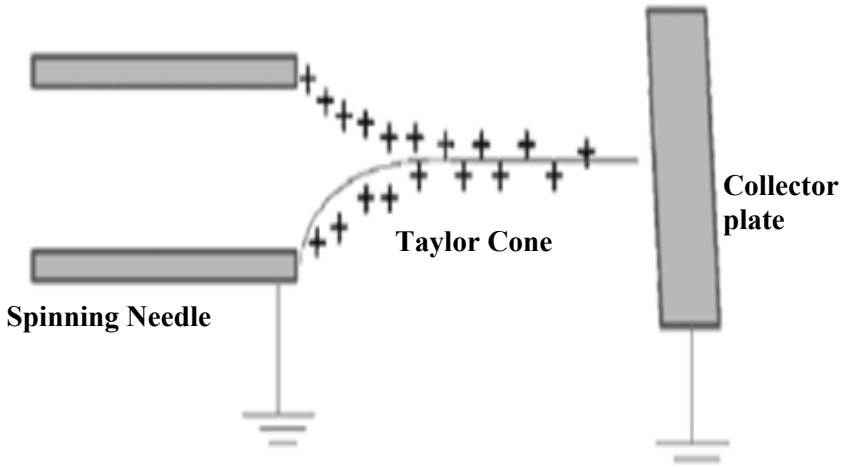

Figure 3.2: Taylor cone formation during electrospinning. When voltage is increased to overcome the surface charge, a jet is ejected from the apex of the spinneret to form the taylor cone [107].

There are several other spinning methods than can be used and they are drawing, template synthesis, phase separation and self-assembly [108-110]. Although each has its own advantages, electrospinning remains the most flexible because of ease of control over the morphology, orientation and size of the nanofibers. Parameters that can affect morphology, size and shape of the nanofibers are charge density, distance of nozzle to the collector, jet radius, solution viscosity, surface tension and humidity. Furthermore, depending on the parameters, nanofibers can have a variety of morphologies which can be smooth, beaded, hollow, rods, ribbons, wires or porous [111]. For characterisation, scanning and transmission electron microscopy (SEM and TEM) are commonly used to observe their surfaces.

3.3 Electrospun nanofiber point of care colorimetric probes for detection of Alkaline Phosphatase for diagnosis of liver toxicity

The challenges encountered during diagnosis of liver toxicity in telemedicine as discussed in chapter 2 have presented an urgent need to develop a simple point of care probe for detection of ALP. However, in order for any probe to be suitable, it must be cost effective, sensitive to the analytes of interest, user-friendly, rapid, robust, equipment free and easily deliverable.

Electrospun nanofibers have therefore shown to meet these criteria in the following ways. Firstly, from a cost point of view, polymer materials and standard colorimetric substrates are cheap. Secondly, the good affinity of the immobilised substrates to ALP makes the probe to

be sensitive and specific. Thirdly, since detection relies on visual colour changes, this makes for a user-friendly probe that even unskilled personnel can operate. Furthermore, the probe can be modified to be a self-integrated device capable of sample preparation, separation and detection. Lastly, delivery of the device to resource poor settings can be achieved with ease since the probe is portable and instrumentation is not required.

An example of such a self-integrated colorimetric probe was designed by Vella and co-workers [19]. Even though they used bioactive paper as the solid support for the substrates instead of nanofibers, the principles of operation would be the same. Their colorimetric probe was for detection of ALP, Aspartate aminotransferase (AST) and serum proteins for liver function tests. The diagnosis procedure is illustrated in Fig. 3.3. The blood would first be sampled from the suspected patient using a pin to stick the finger to produce enough sample of between 10-20 μL. Then, the droplet would be placed on the topside of the device for vertical flow filtration so as to produce plasma which would react with the substrates in the three test zones. The elevated presence of ALP, AST and serum proteins would then be expected to change colours of the test zones from white, dark blue and yellow to dark purple, pink and green respectively. The colours changes would be viewed from the bottom side of the device.

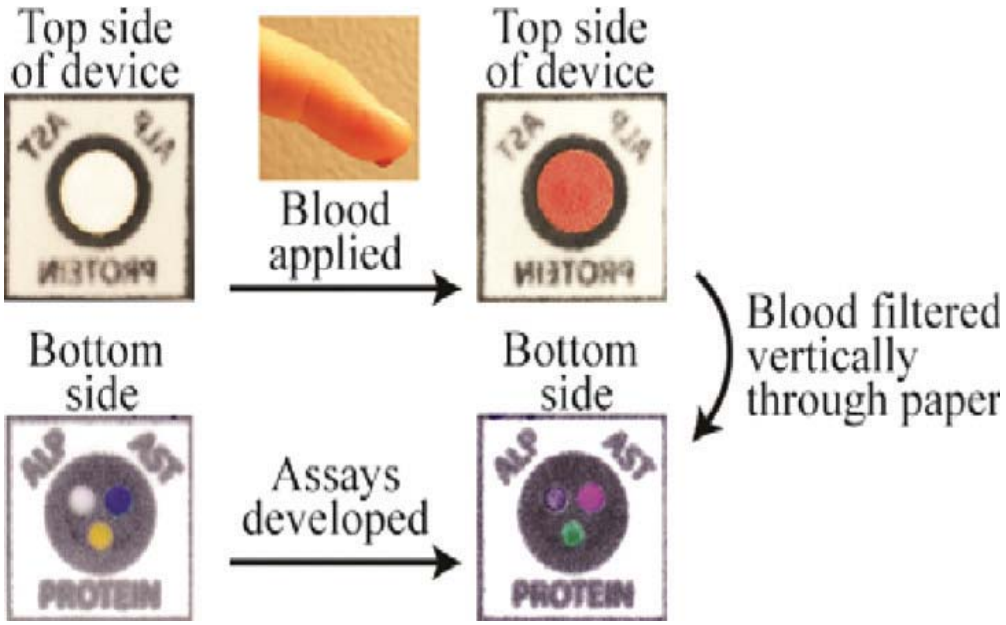

Figure 3.3: Bioactive paper colorimetric probe procedure for diagnosis of liver toxicity. The diagnosis procedure involves sampling of the suspected patient

followed by vertical flow of the blood to the test sites. Then elevated levels of ALP, AST and serum proteins would be expected to turn the test zones from white, dark blue and yellow to purple, pink and green respectively [19].

The only difference between bioactive paper and electrospun nanofibers would be that in the latter, not only can substrates be physisorbed but they can also be chemisorbed. The advantage of chemisorption is that its strong covalent bonds can prevent leaching of substrates compared to the weak dispersion forces (less than 5 % of the strength of covalent bond) of physisorption [112]. Therefore, electrospun nanofibers would be considered to have a more competitive edge over bioactive paper in this sense. However, since no work has been reported on the use of electrospun nanofibers as colorimetric probes for detection ALP, an example of colorimetric polydiacetylene (PDA) electrospun nanofibers will be used to illustrate how nanofibers can be used to detect ALP.

Polydiacetylene (PDA) is an optical polymer formed by polymerization of 1. 4 addition of diacetylenic monomers which is initiated by Ultra Violet (UV) irradiation. The polymer exhibits chromatic changes to a blue colour (650 nm) after polymerization and a red colour (540 nm) upon interaction with stimuli such as temperature, pH and biomolecules [113]. Electrospinning of PDA was first reported by Kim and co-workers and they used top-down and bottom-up methods for polymerization [114]. The scheme in Fig. 3.4 shows their bottom up approach whereby several polymer matrices were mixed with PDA monomers (diacetylenes) in organic solvents. During electrospinning, the solvents evaporated and the monomers self-assembled themselves as can be seen in the figure. When UV was irradiated on the white nanofibers, they turned to the expected colour of blue (Fig. 3.5) which indicated that molecular property of the monomers was not lost. Then exposure of the nanofibers to the analytes of interest turned them from blue to red (Fig. 3.5) as expected.

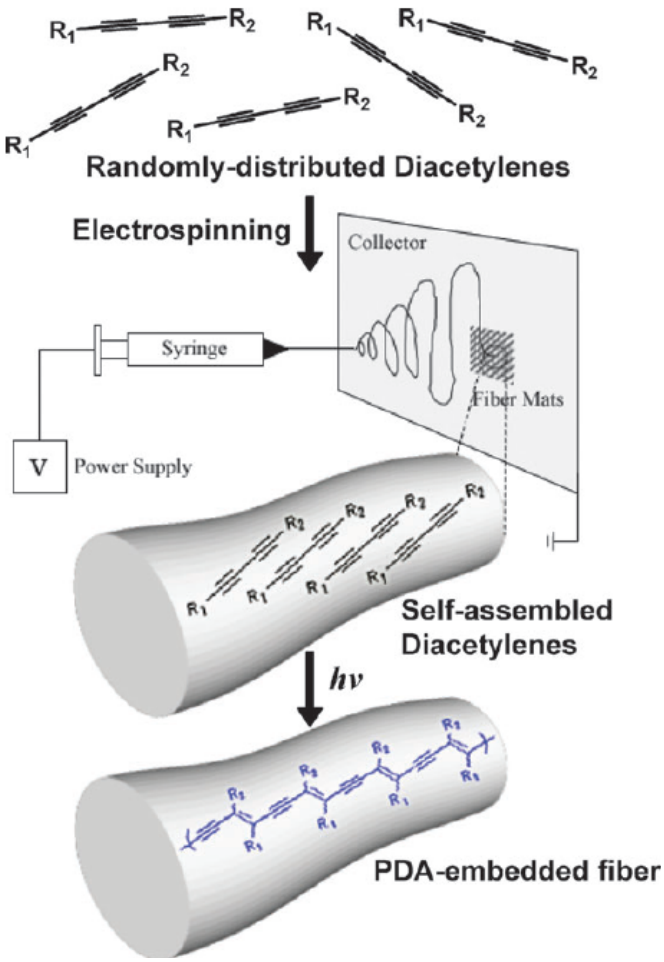

Figure 3.4: Electrospinning of polymer nanofiber embedded with PDA. The polymer is firstly electrospun followed by irradiation with UV light (254 nm) to initiate polymerization [114].

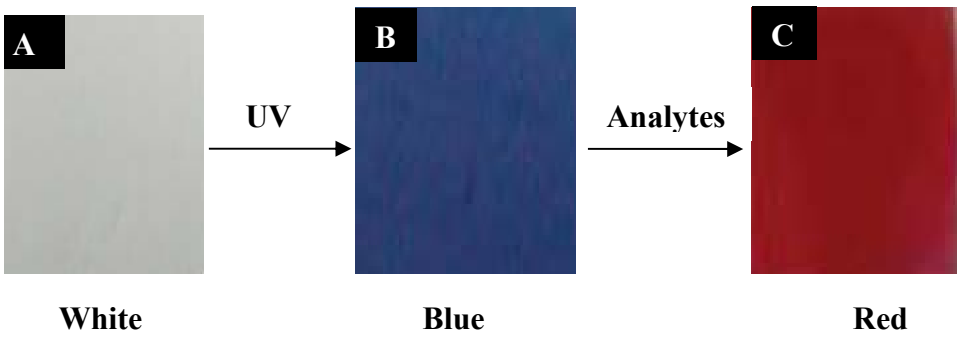

Figure 3.5: Colour changes associated with PDA electrospun nanofibers. The mat remains white after electrospinning (a) but turns blue when irradiated with UV (b). Exposure to analytes can further change the mat from blue to red (c) [115].

Although no work has been reported where PDA has been used to detect ALP, the colour changes expected would be similar if the polymer was functionalised with a phosphoserly group. The hypothetical illustration is shown in Fig. 3.6. The colour would be expected to turn from blue to red upon hydrolysis of the phosphoserly by ALP. However, since most polymers are not intrinsically colorimetric in nature like PDA, colorimetric substrates immobilised would be the ones responsible for the colour changes.

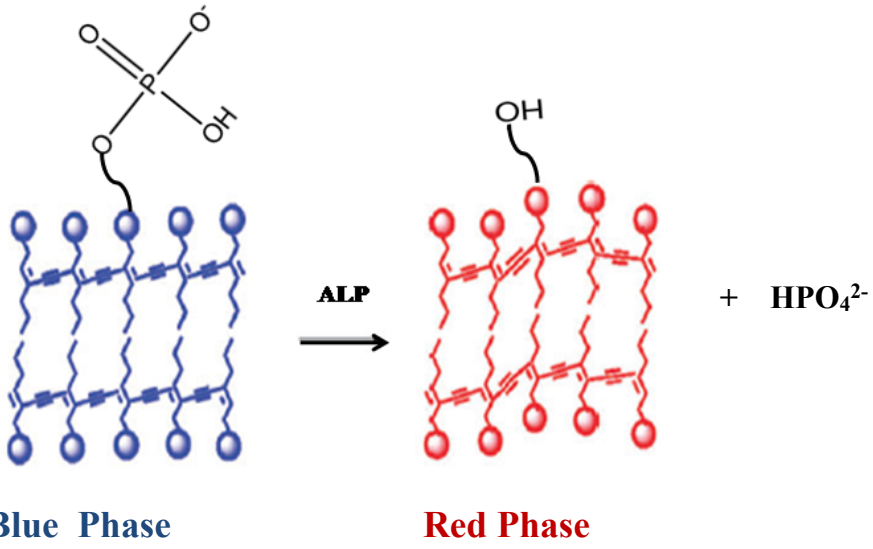

Figure 3.6: Phosphate functionalised PDA backbone for colorimetric detection of ALP. Hydrolysis of the phosphate monoester bond can change the colour from blue to red.

In summary, electrospun nanofibers exhibit unique properties that present them as suitable point of care colorimetric probes for the detection of ALP for diagnosis of liver toxicity. Their ability to be incorporated into analytical devices means diagnosis can be carried out even by unskilled personnel since sample preparation, separation and detection are all integrated into the device. Further, the device can also be delivered with ease to resource poor settings because it is portable and does not require heavy instrumentation. Therefore, the objectives of the research work and the scope of the thesis will be presented since all the objectives could not be achieved due to time limitations.

3.4 Objectives of the thesis

The driving force in the project was to design a novel self-integrated electrospun nanofiber colorimetric probe for detection of ALP for diagnosis of liver toxicity. The proposed features of the probe are shown in Fig. 3.7. They are a pall plasma filter (for removal of red blood cells), a buffer compartment (for dilution of the plasma to remove interferences) and a pNPP immobilised nylon electrospun nanofibers (to act as platforms for detection of ALP). The plasma filter operates by a size exclusion mechanism whereby the pore sizes at the top of the membrane are approximately 50X larger than at the bottom (100 μm to 2μm) of the filter [116]. Then as blood vertically flows through the membrane, the red blood cells partway through the cross-section without clogging the pores. Plasma can then flow through to the bottom of the filter until it reaches the test zone. Nylon was chosen for its mechanical strength and pNPP for being the standard substrate used in routine diagnosis of liver toxicity. Therefore, the rationale was that once the blood was filtered, the elevated levels of ALP in the plasma would hydrolyse pNPP and white nanofiber mats would turn to a yellow colour. The intensity of the colour would be directly proportional to the activity of ALP. Furthermore, the device would rely on vertical flow since large sample volumes would not be required.

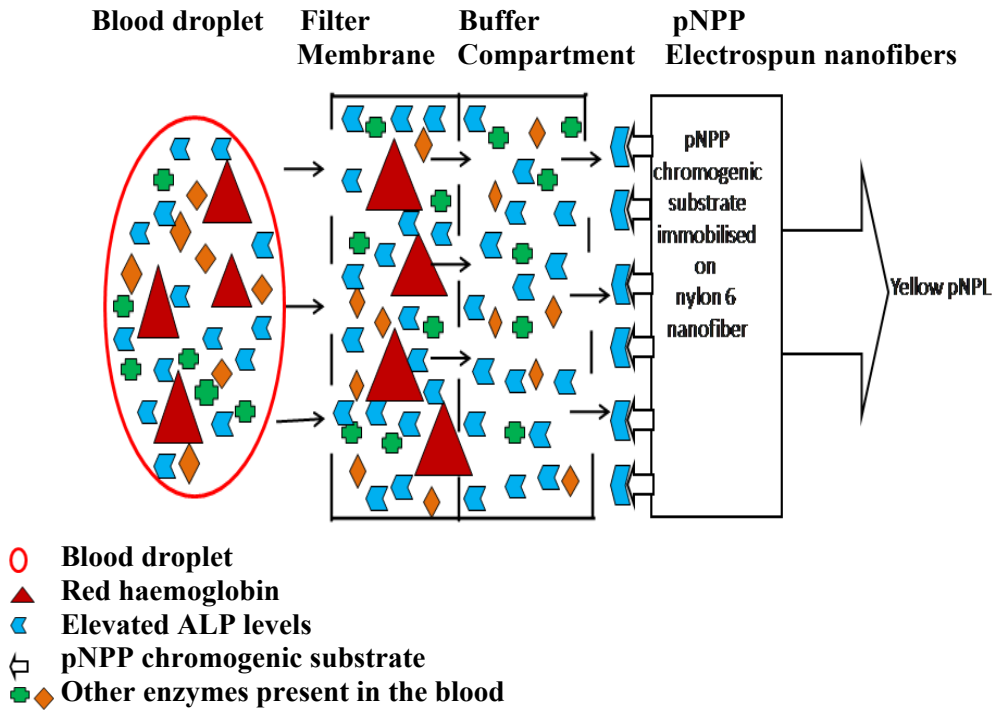

Figure 3.7: Electrospun nanofiber based colorimetric device for detection of ALP for diagnosis of liver toxicity. The probe would operate by vertical filtration of blood to produce plasma which would be diluted before flowing to the electrospun nanofibers immobilised with pNPP. The yellow colour of pNPL product would be expected to intensify with increase in the levels of ALP.

For the scope of the thesis, the focus was to synthesise nylon electrospun nanofibers immobilised with pNPP and use them as colorimetric probes to detect ALP. To eliminate blood sample preparation and separation steps, biological samples of ALP were purchased. The objectives were as follows; to characterise ALP in solution using Michaelis Menten and Lineweaver Burk kinetics models, to assay ALP in solution, to synthesise nylon-pNPP electrospun nanofiber composites and to employ them as colorimetric probes for the detection of ALP.

Chapter 4

4. Experimental

4.1 Materials

Tris (hydroxymethyl) aminomethane base ($NH_2C(CH_2OH)_3$), ethylenediaminetetraacetic acid disodium (EDTA) ($C_{10}H_{14}N_2Na_2O_8 \cdot 2H_2O$), sodium carbonate ($Na_2CO_3$), para nitrophenyl phosphate disodium salt hexahydrate (pNPP) ($O_2NC_6H_4OP(O)(ONa)_2 \cdot 6H_2O$), para nitrophenol (pNP) ($O_2NC_6H_4OH$), calcium chloride ($CaCl_2$) and nylon 6 (M_w = 10,000), all of purity more than 95 %, were purchased from Sigma-Aldrich (South Africa). All reagents were of analytical or high performance liquid chromatography (HPLC) grade. Hydrochloric (HCl) (37 % v/v), formic and glacial acetic (HAc) acid concentrates were also purchased from Sigma-Aldrich. The ALP purchased from Sigma-Aldrich was from *E.coli* (ammonium sulfate suspension, 30-90 units/mg protein (modified warburg-christian in glycine buffer), 3.25 mg protein/ml and 62.77 units/mg protein). Tris-HCl (0.5 M, pH 7.4) mixed with 1 mM of calcium chloride ($CaCl_2$) in deionized water was used as the assay buffer. 33 mM EDTA and 20 mM sodium carbonate dissolved in Tris-HCl (0.5 M, pH 9) solution was used as the stop buffer. ALP and pNPP stock solutions were prepared with the assay buffer. Human serum type AB (male) from male AB was also purchased from Sigma-Aldrich.

4.2 Evaluation of chemical stability of para nitrophenyl phosphate and para nitrophenol in various pH conditions

The purpose of evaluating pNPP and pNP was to confirm their chemical stability by checking whether they would behave as expected in acidic, biological and alkaline pH mediums. Both pNPP and pNP are known to be colourless under biological and acidic pH conditions respectively while deprotonation of pNP in alkaline conditions forms pNPL which is yellow in colour. A stock solution of pNPP (0.06 mM) was prepared in the assay buffer (pH 7.4) while two stock solutions of pNP (0.06 mM) were prepared in 1 M HCl (pH 2) and also in 0.5 M Tris-HCl (pH 9). The three samples were analysed using a scanning UV/Visible (UV/Vis) spectrophotometer to determine their maximum wavelength absorbance. Their spectra were normalized for comparison. Furthermore, the molar extinction coefficient (ε) of pNPL was determined by preparing standards of 0, 0.01, 0.02, 0.03, 0.04, 0.05 mM which were scanned from 250 to 500 nm to determine their maximum wavelength absorbance. Concentrations of

the standards were then plotted against their absorbance and the equation of the line determined. The slope of the equation would be equivalent to the molar extinction coefficient (ε) derived from beer lambert law which is given as A=εcl (A, absorbance at maximum wavelength (y); ε, molar extinction coefficient (m); c, dye concentration (x); l, length of light path).

4.3 Preparation of para nitrophenolate calibration curve

A calibration curve for pNPL using a 96 well plate was prepared to convert absorbance into concentration of products formed during enzyme kinetics and assay studies. A stock of 1 mM was prepared with the assay buffer and standards of 0, 200, 300, 400, 600, 800 and 1000 μM (0, 0.02, 0.04, 0.06, 0.08, and 0.01 μmoles respectively) were aliquot in triplicates into the wells. Then a stop buffer was added to mimic the conditions in which the product would form during enzyme kinetics and assaying experiments. Absorbance was monitored at 405 nm using a plate reader UV/Vis spectrophotometer.

4.4 Enzyme kinetics studies of Alkaline Phophatase

V_{max} and K_m enzyme kinetics parameters were determined using Michaelis Menten and Lineweaver Burk plots. A stock solution of pNPP (0.1 mM) was prepared in the assay buffer and standards (0, 0.02, 0.04, 0.06, 0.08, 0.1 mM) were aliquot in a 96 well plate. The reaction was initiated by adding a constant concentration of ALP free enzyme (0.5 μg/ml). The time allowed for the reaction to proceed was 1 min at a temperature of 25 °C. Then 110 μL of stop buffer was added to terminate the reaction and measurements were taken immediately using the plate reader. The experiments were carried out in triplicates and pNPL calibration curve was used to convert absorbance into rates for the kinetics to be plotted.

4.5 Solution state assaying of Alkaline Phosphatase

Free ALP enzyme activity (IU/L) was determined by preparing standards (0, 2, 4, 6, 8, 10 μg/ml) in the assay buffer and assaying for 1 min at 25 °C. The substrate was kept constant at a concentration of 1 mM. Once the reaction time came to an end, the stop buffer (110 μL) was added and absorbance was evaluated at 405 nm using a UV/Vis plate reader. The pNPL standard curve was used to convert absorbance into activity (IU/L). The enzyme activity was also determined in crude and 10x diluted serum samples (in assay buffer) which were both

spiked with ALP. 40 μg/ml of ALP was diluted 2x with each of the two serum samples and standards of 0, 2, 4, 6, 8, 10 μg/ml assayed.

4.6 Synthesis of electrospun nylon-para nitrophenyl phosphate nanofiber composites

Electrospun nanofibers were synthesised by blending 5.6 mM of pNPP with 16 % nylon 6 in 10 ml formic/acetic acids (1:1 v/v). The solution was stirred for 12 h while covered with aluminium foil to prevent exposure to light. The polymer solution was loaded onto a 10 ml syringe and mounted on a programmable syringe pump (New Era, NE-1000). The electrospinning conditions were rate flow of 0.5 ml/h, voltage of 21 kV and working distance of 15 cm.

4.7 Solid state assaying of Alkaline Phosphatase on nylon-para nitrophenyl phosphate nanofibers

Nylon-pNPP nanofiber composites were used as platforms for assaying of free ALP. 20 μL of enzyme standards (0, 2, 4, 6, 8, 10 μg/ml) were aliquot unto precut fiber mats (0.5 cm x 0.5 cm) and the yellow colour formation monitored over a 5 min period. The same procedure was also carried out using 10x diluted serum samples spiked with ALP.

4.8 Leaching of para nitrophenyl phosphate from the electrospun nanofibers layer

To determine the rate of pNPP leaching into solution, a composite mat (0.5 cm x 0.5 cm) was dipped in 500 μL of the assay buffer. Samples of 50 μL were taken at 0.25 min intervals for 2.5 min and absorbance read at 305 nm using a plate reader. The rate of leaching was determined by dividing absorbance by time. The experiment was carried out in triplicates.

4.9 Effect of heat on the chemical stability of nylon-para nitrophenyl phosphate nanofiber composites

The nanofiber mats were heated up for 12 h at 40 and 80 ºC and used to assay for free ALP as described in section 4.7.

4.10 Characterization of solution and nanofibers experiments

The chemical stability evaluation of pNPP and pNP under various pH conditions and nylon-pNPP polymer solution were characterized using Perkin Elmer Lambda 25 UV/Vis spectrophotometer. All the other experiments were analysed with Power Wavex UV/Vis plate

reader spectrophotometer. Morphology of the fibers was observed on Vegan Tescan (TS5136ML) scanning electron microscope (Brno, Czech Republic).

Chapter 5

5. Results and Discussion

5.1 Evaluation of chemical stability of para nitrophenyl phosphate and para nitrophenol in various pH conditions

The results showed that pNPP and pNP were colourless in biological pH of 7.4 and acidic pH of 2 respectively (Fig. 5.1a). This was confirmed by the absorption bands in the UV region. The maximum absorption band for pNPP was 305 nm and 317 nm for pNP (Fig. 5.1b). There was also a yellow colour formation for pNPL in alkaline conditions (pH 9) while absorption was in the visible region with maximum band at 405 nm (Fig. 5.1a and 5.1b).

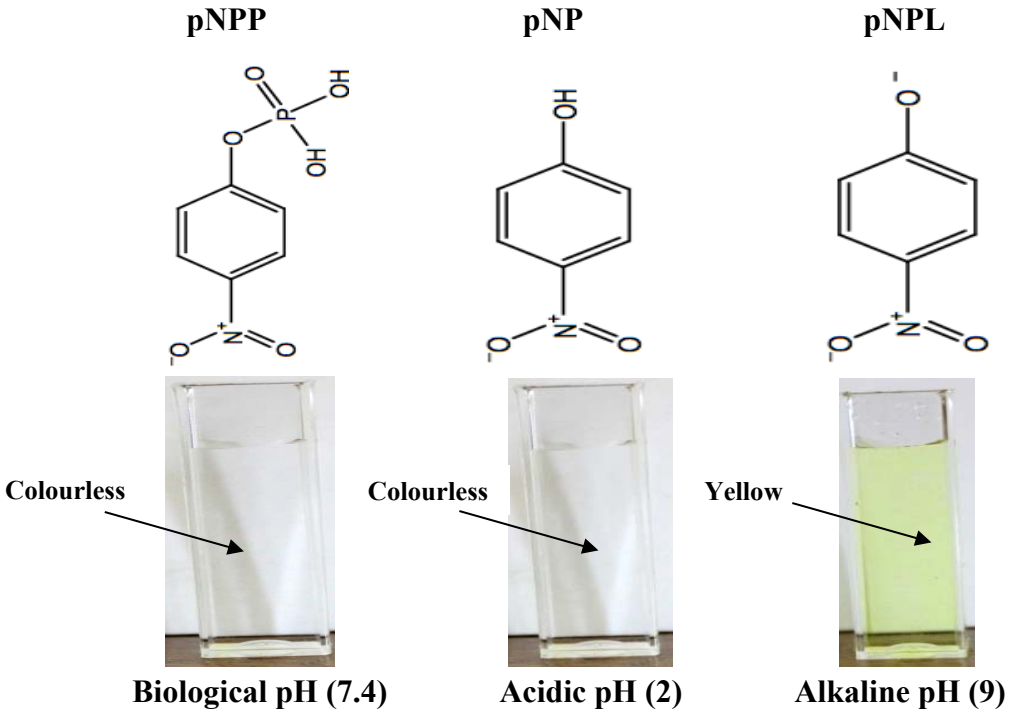

Figure 5.1a: Colours associated with pNPP, pNP and pNPL under biological, acidic and alkaline pH conditions, respectively. pNPP and pNP were colourless in biological pH (7.4) and acidic pH (2) respectively. pNPL was yellow in alkaline pH (9).

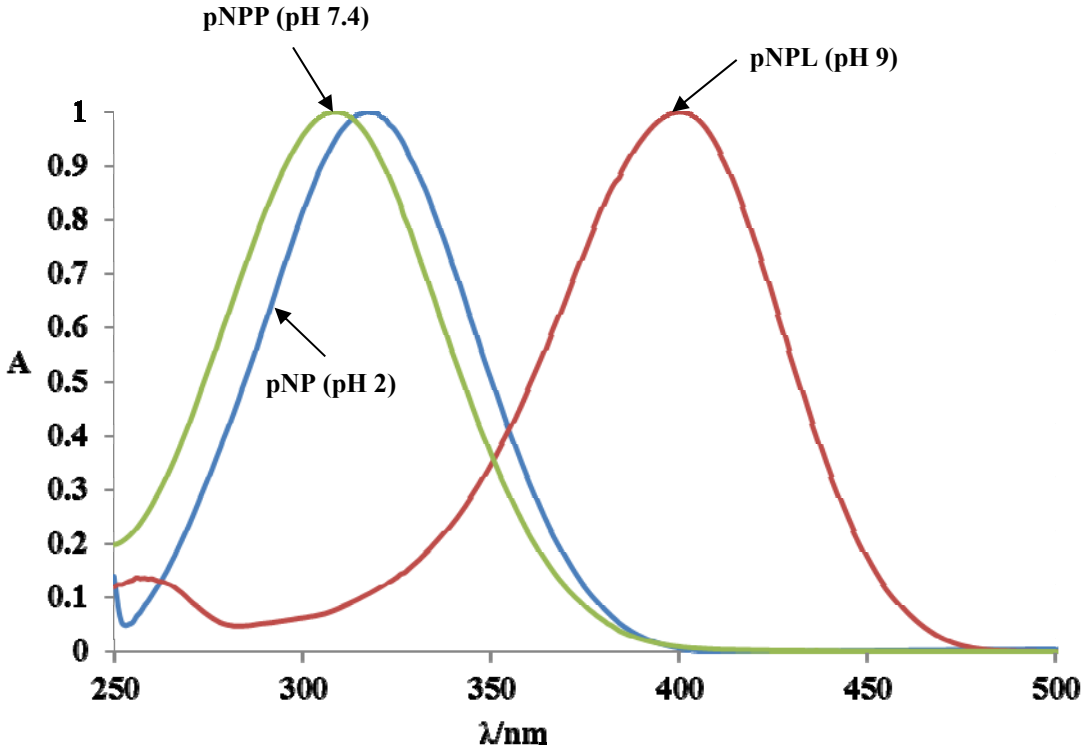

Figure 5.1b: UV/Vis spectra of pNPP, pNP and pNPL. The substrate of pNPP (305 nm) and product of pNP (317 nm) both absorbed in the UV region while pNPL (405 nm) absorbed in the visible region.

The observed UV absorption bands for pNPP and pNP were a result of charge transfer and π-π* interactions between the aromatic ring π electron acceptors and nitro group π electron donors [117]. The band at 405 nm and the yellow colour observed for pNPL in alkaline conditions was due to deprotonation of the phenol's hydroxyl group (OH). Removal of the proton results in π electrons resonance in which the bond order between nitrogen and oxygen decreases while the one between nitrogen and carbon increases [118]. This causes a bathochromic shift as the molecules absorb at longer wavelengths in the visible region. Therefore, the results confirmed that the reagents were chemically stable since they behaved as expected under various pH conditions and could be used for further studies.

The spectra of the standards prepared for determining the molar extinction coefficient (ε) of pNPL showed an increase in absorbance at 405 nm as concentration also increased (Fig. 5.2). A plot of concentration against absorbance showed a linear correlation between the two because the regression analysis value was 0.999 (data not shown). The slope of the equation was equal to the molar extinction coefficient (ε) calculated to be 18,458 M^{-1} cm^{-1} which was close to 18,400 M^{-1} cm^{-1} reported in literature [46-47].

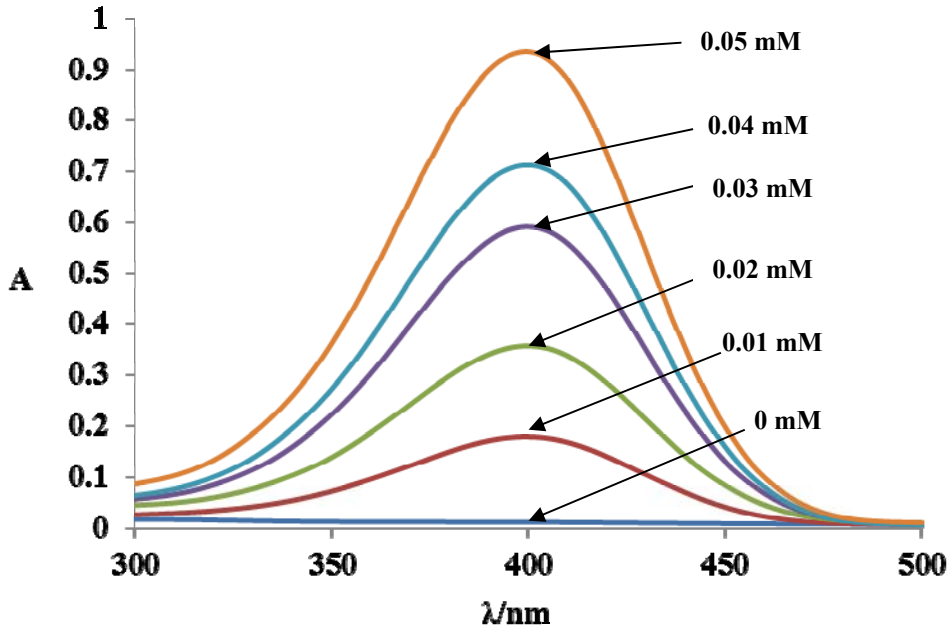

Figure 5.2: UV/Vis spectra of pNPL standards at lambda maximum of 405 nm. There was a linear increase in absorbance with increase in concentration.

Molar extinction coefficient (ε) was important to determine due to the fact that it is a characteristic parameter of any chromophore. Compounds with a value above 10,000 M^{-1} cm^{-1} are normally considered to have a strong chromophore because of the π-π* transitions and charge transfers [119]. However, the slightly higher value of 18,458 M^{-1} cm^{-1} obtained compared to 18,400 M^{-1} cm^{-1} reported in literature could have been due to solvent effects. Polar solvents such water contain OH auxochromes that tend to modify the absorption of a chromophore. The lone pairs on the OH solvates the chromophore which can lower the transition energy between the π-π*. The decrease in energy can lead to an even further bathchromic or red shift which causes the chromophore to absorb more light energy [120]. Nonetheless, pNPL did possess a strong chromophore suitable to be used in ALP kinetics and assay studies.

In summary, pNPP and pNP were chemically stable in biological pH (7.4) and acidic pH (2) respectively. In addition, a yellow coloured product of pNPL was produced under alkaline conditions (pH 9) due to the deprotonation of pNP which further confirmed the chemical stability of pNP. The molar extinction coefficient (ε) of pNPL was 18,458 M^{-1} cm^{-1} which was close to 18,400 M^{-1} cm^{-1} reported in literature. The results confirmed that the reagents were chemically stable under different pH mediums and could be used for further studies.

5.2 Enzyme kinetics of Alkaline Phosphatase

Evaluation of the calibration curve for pNPL showed that there was an increase in absorbance with increase in the number of moles (µmol). The regression equation of the line was y=14.369x + 0.0113 (data not shown). The line of perfect fit showed a linear correlation between the two parameters as regression (R^2) was 0.999. To plot Michaelis Menten (MM) (Fig. 5.3) using this equation, absorbance was converted to µmol and divided by the 1 min reaction time to determine the rates of the reaction (µmol/min^{-1}). Then, pNPP substrate concentrations (mM) were plotted against these rates to determine the kinetic parameters. Lineweaver Burk (LB) (Fig. 5.4) was plotted as a double reciprocal of the linear portion of MM.

MM plot showed a V_{max} of 5×10^{-3} µmol/min^{-1} and a K_m of 0.026 mM while LB had a V_{max}, K_m and K_m/V_{max} of 5.5×10^{-3} µmol/min^{-1}, 0.025 mM and 4.5 mM/µmol/min^{-1} respectively. Excess substrate concentration (10x K_m) on MM and LB were determined as 0.26 and 0.25 mM respectively.

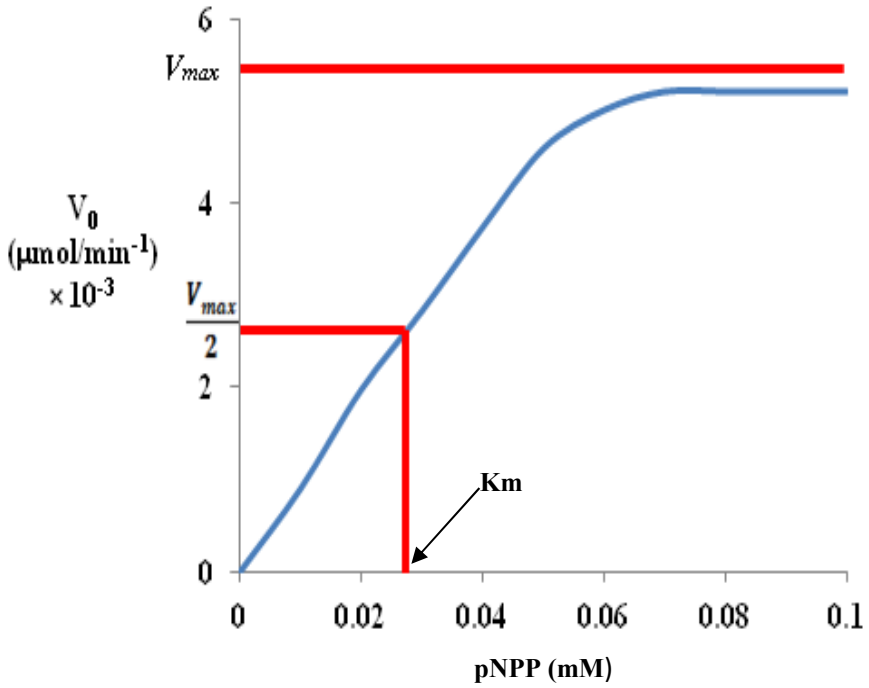

Figure 5.3: Michaelis Menten curve of ALP. V_{max} and K_m were determined to be 5×10^{-3} µmol/min^{-1} and 0.026 mM respectively.

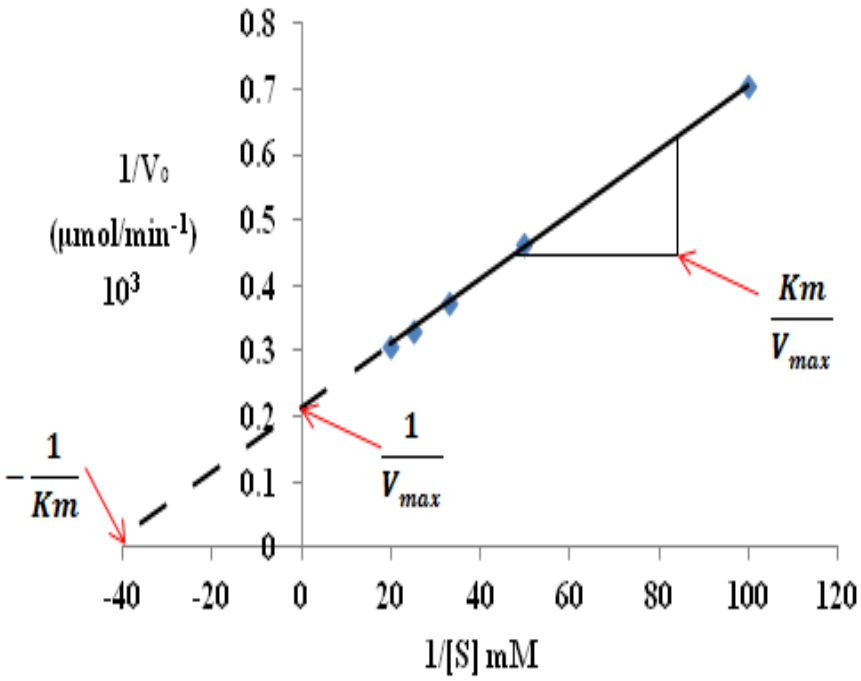

Figure 5.4: Lineweaver Burk of ALP. The V_{max}, K_m and K_m/V_{max} were 5.5×10^{-3} µmol/min^{-1}, 0.025 mM and 4.5 mM/µmol/min^{-1}.

LB is a more accurate measure of V_{max} and K_m because it gives greater emphasis to the points at low concentrations which are susceptible to errors. MM on the other hand is usually prone to errors due to the difficulty in experimentally measuring the initial rate of the reaction at high substrate concentrations [38]. However, between the two plots, there were no significant differences in the two parameters. V_{max} was reached at high pNPP concentration because the active sites of ALP were fully saturated as they were all converted to enzyme-substrate (ES) complexes [121]. A plateau at V_{max} was also reached because the rate of the reaction had become insensitive to increase in pNPP concentration as can be observed from 0.06 mM pNPP concentration on the MM plot.

Furthermore, the plateau indicated that ES maintained a steady state since the rate of complex synthesis was equal to the rate of substrate consumption. The steady state can be maintained until the substrate is nearly exhausted. Therefore, it was deduced that the reaction followed a zero order with respect to pNPP concentration as would be expected in MM kinetics [121]. However, despite the valuable information obtained on MM plot about enzyme-substrate interactions, one of its drawbacks is that the extrapolated value of V_{max} can never be accurately determined even at excess substrate concentrations. This is because the maximum

rate of the reaction (v_o) is usually 91 % of V_{max} [121] hence the reason LB is a better method for determining V_{max} and K_m.

The K_m value (2.5×10^{-2} mM) measured on the LB plot, was significant as it indicated that ALP had a good affinity for pNPP. K_m values in the range of 10^{-2} and 10^{-5} are normally considered to show a strong binding between an enzyme and its substrate [40]. In fact, the lower the K_m value, the greater the enzyme-substrate affinity since this implies the enzyme can achieve maximum catalytic efficiency even at lower substrate concentrations. Furthermore, K_m was also important in determining the excess substrate concentration (0.25 mM) that would be required to ensure the enzyme does not run out of substrate during solution and solid state assaying of ALP.

Therefore, to summarise the results, the kinetics parameter of K_m was useful in showing that ALP had a good affinity to pNPP. In addition, the excess substrate concentration determined using K_m was also valuable in indicating that pNPP concentration should be above 0.25 mM to ensure that the enzyme does not run out of substrate in solution and solid state assaying.

5.3 Solution state assaying of free Alkaline Phosphatase

Enzyme activity standard curve for free ALP (Fig. 5.5) was prepared by plotting enzyme concentration (µg/ml) against enzyme activity (IU/L). The enzyme activity was obtained by dividing the rate (µmol/min^{-1}) with the sample volume (L). Activity increased in a linear fashion ($R^2 = 0.984$) with increase in enzyme concentration. There was also an increase in the yellow colour intensity formation as shown in Fig. 5.6. Enzyme activity for each standard (0, 2, 4, 6, 8, 10 µg/ml) was calculated to be 0, 191, 376, 546, 700, 858 IU/L respectively.

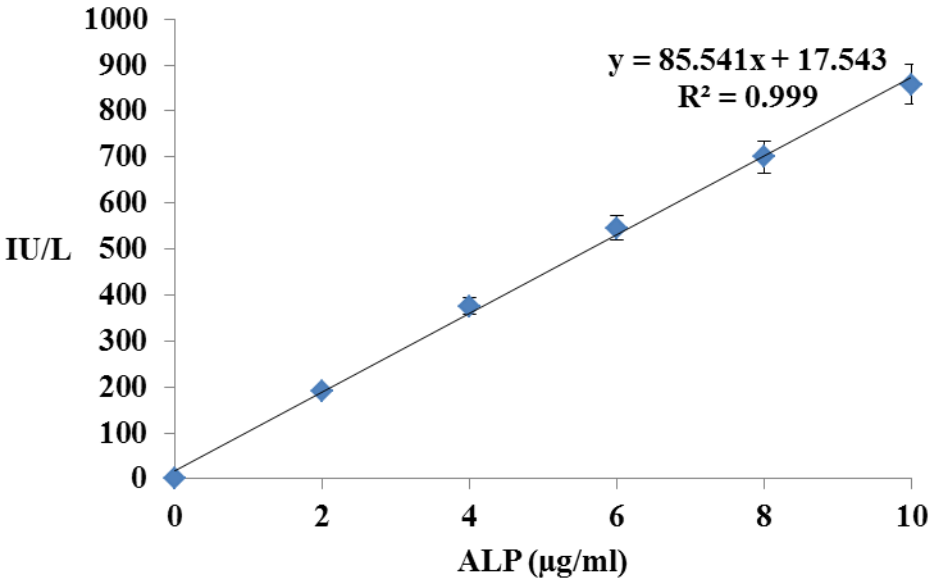

Figure 5.5: Enzyme assaying standard curve of ALP free enzyme. Enzyme activity increased with increase in enzyme concentration. The samples were ran in triplicates and the error bars represent a 95 % confidence interval.

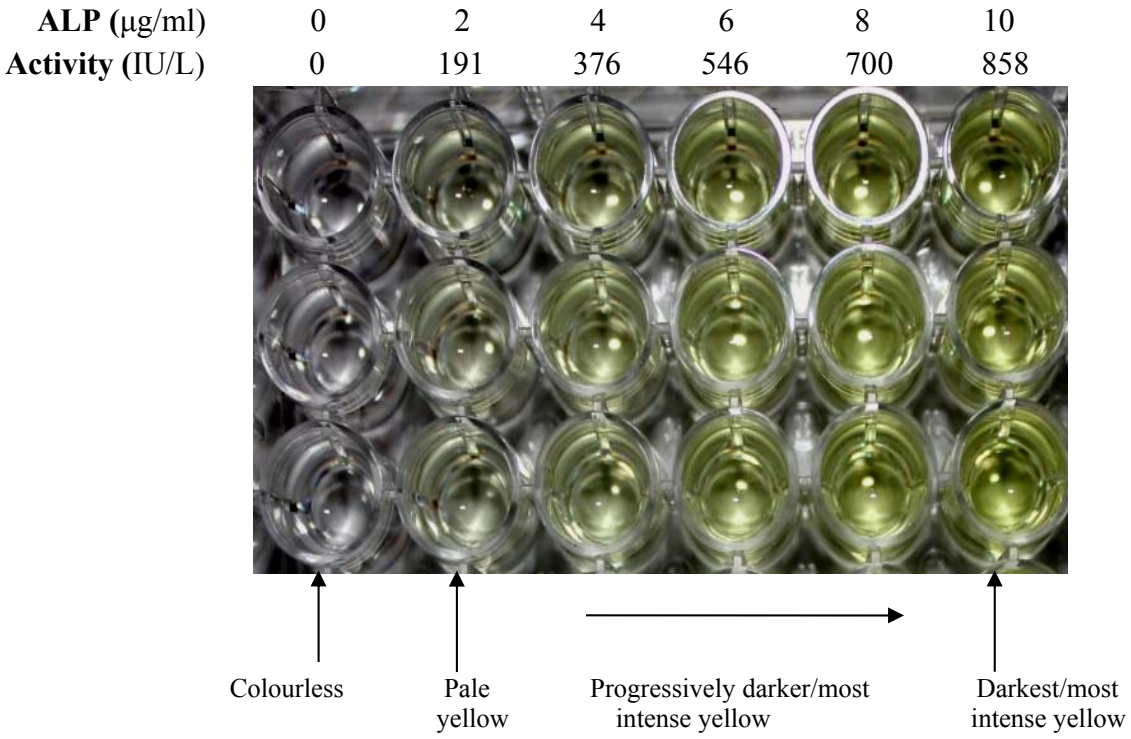

Figure 5.6: Yellow colour intensities associated with assaying of free ALP enzyme. The experiments were carried out in triplicates and the yellow colour intensified with increase in enzyme activity.

The yellow colour intensities observed after 1 min indicated that the kinetics were extremely fast due to good ALP affinity to pNPP as already established using MM and LB plots. At low ALP concentration of 2 µg/ml, there was not enough enzyme to convert all the substrate into product within the 1 min reaction time hence the faint yellow colour. However, at 10 µg/ml, the rate of the reaction was faster since there were more enzyme molecules forming product hence the deep yellow colour observed within the same reaction time. Therefore, the results showed that enzyme concentration was directly proportional to activity. They also indicated that the enzyme was highly active since usually inactive enzyme (due to denaturation for instance) does not show increase in activity even at high concentrations.

The upper limit of normal for ALP activity is ≤ 120 IU/L while elevated levels due to liver toxicity can rise up to 10 times this limit. The desired feature of the probe is for the yellow colour to only form above this level. This means the limit of detection (LOD) should be at 120 IU/L. For this assay, the LOD was 73 IU/L which was 47 units below the 120 IU/L. However, even though it was spectrophometrically lower than the desired value, the faint yellow observed at 191 IU/L indicated that at 120 IU/L the colour would be even fainter which would still be acceptable considering that the probe is meant to be qualitative.

Enzyme activity could not be measured beyond 858 IU/L because of limitations on the spectrophotometer and so the method could only detect up to 7.15x the upper limit of normal (858 IU/L ÷ 120 IU/L = 7.15). The limitation of the spectrophotometer was that it was calibrated up to a maximum absorbance of 4 which correlated to the maximum absorbance obtained for pNPL calibration curve used to convert assay readings to activity. Therefore, it would have been preferable to detect up to at least 10x since in severe liver damage, ALP can rise up to 1200 IU/L which is 10x the normal limit. However, despite the limitations, the results were useful in establishing enzyme concentrations that corresponded to certain activities. Being able to correlate enzyme concentrations to activities is helpful in translating assaying into solid state because one would know how much enzyme to add to obtain a certain activity.

In summary, the observations on the enzyme activity standard curve indicated that the enzyme was highly active as enzyme concentration increased with activity. The LOD of 73 IU/L was still acceptable even though it was not at the 120 IU/L upper limit of normal. Furthermore, the

faint yellow colour observed at 191 IU/L indicated that the colour would not be visible at 120 IU/L as this would be ideal to prevent misdiagnosis. Lastly, the method could only detect up to 7.15x the upper limit of normal due to limitations of the spectrophotometer.

5.4 Solution state assaying of serum spiked with Alkaline Phosphatase

A crude serum sample was purchased because blood sample preparation by filtration to obtain plasma was outside the scope of the thesis. Moreover, plasma prepared by centrifugation of blood could not be used because it contained anticoagulants which inhibited ALP. Therefore, serum was the best alternative since it is essentially plasma without clotting factors and it is also the standard sample of preference in routine clinical diagnosis of liver toxicity in laboratories. However, even though serum is not the appropriate sample matrix for the colorimetric device, the findings from this experiment would still be valuable in predicting how the assay method would work when the appropriate plasma is eventually used. Serum was spiked with ALP because a diseased patient's sample could not be obtained due to ethical reasons.

The results of crude serum spiked with ALP are shown in Fig. 5.7a and 5.7b. It can be seen that the assay did not induce any formation of the yellow colour. However, an increase in absorbance was still observed even though there was no colour formation. This indicated there were interferences in the serum that absorbed at the same wavelength as pNPL. The absorbance signals were not from hydrolysis of pNPP by the enzyme.

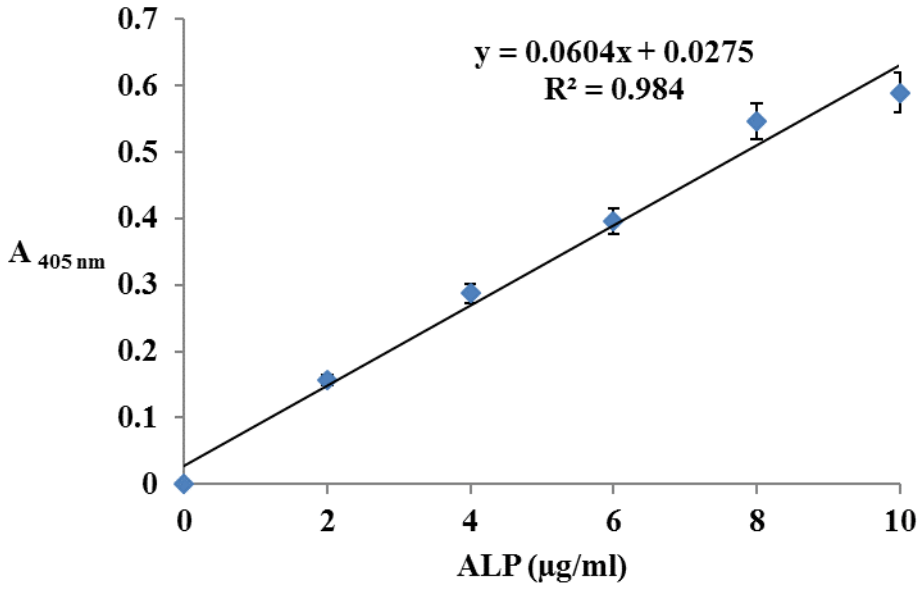

Figure 5.7a: Enzyme assaying standard curve of crude serum spiked with ALP. The absorbance increased with increase in interferences since it was deduced that the readings were not from the formation of pNPL. The results were carried out in triplicates and the error bars represent a 95 % confidence interval.

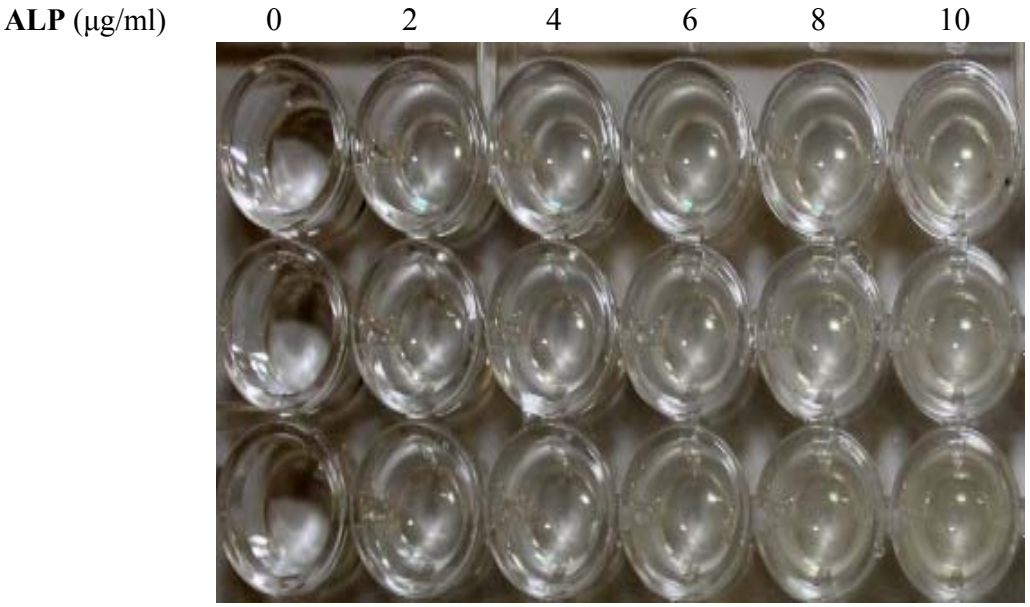

Figure 5.7b: Colourless samples associated with assaying of crude serum spiked with ALP. The experiments were carried out in triplicates and there was no formation of the yellow colour due to interferences.

The interferences were presumed to be from other enzymes, antibodies, minerals, fats, sugars and hormones because they are also found in serum [122]. To confirm that the interferences were the ones responsible for masking the signal of pNPL, serial dilutions (crude, 5x, 10x and 30x) of the crude serum were prepared and ran at 405 nm. The bar graph in Fig. 5.8 shows that absorbance intensity decreased with increase in dilution and this indeed confirmed that interferences in crude sample absorbed at the same wavelength as pNPL. As a result, these observations indicated it would be necessary to dilute the serum in order to bring ALP to detectable levels.

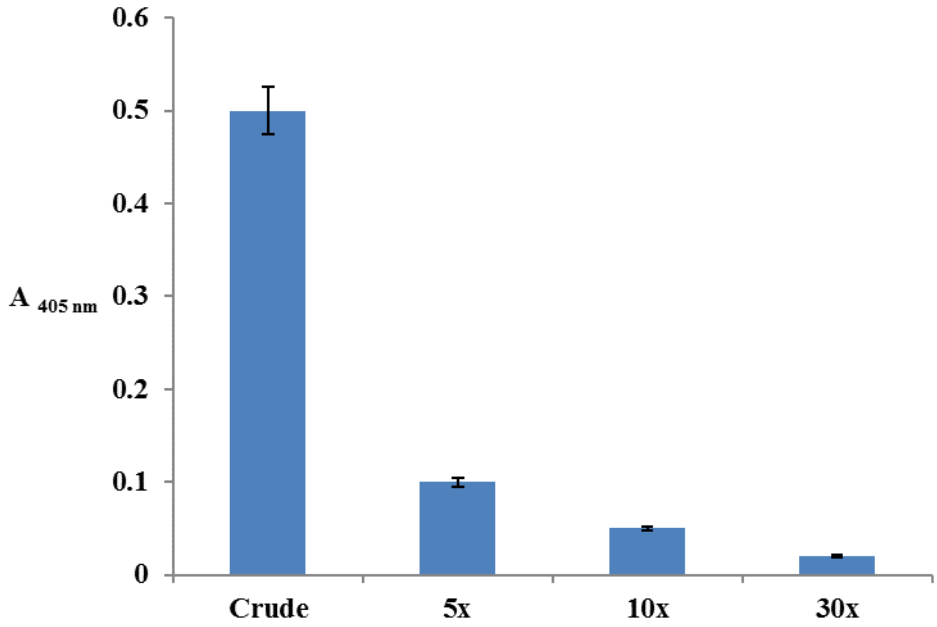

Figure 5.8: Absorbance of serial dilutions of crude serum samples. There was a decrease in interferences as dilution of the crude sample increased. The experiments were carried out in triplicates and the error bars represent a 95 % confidence interval.

With respect to the application of the device, the data was helpful in showing that a buffer compartment should be incorporated to minimise interferences even in plasma. Although Vella and co-workers illustrated that it was possible to detect ALP using crude plasma [19], however, based on the results, we hypothesise that sensitivity of the assay can be further enhanced by diluting the sample. This is because removal of interferences will bring ALP to even higher detectable levels. To test our hypothesis, the serum was first diluted 10x, spiked with ALP and then assayed for enzyme activity.

The results confirmed that indeed dilution resulted in enhanced sensitivity of ALP since formation of the yellow colour could be observed as shown in Fig. 5.9a. Enzyme activity also increased with increase in concentration (Fig. 5.9b). The free ALP enzyme system had enzyme activities of 0, 191, 376, 546, 700 and 858 IU/L while serum activities were 0, 203, 376, 519, 749 and 820 IU /L). There was no significant difference between the two samples although serum assaying could only detect up to 6.84x the upper limit of normal compared to 7.15x for free ALP.

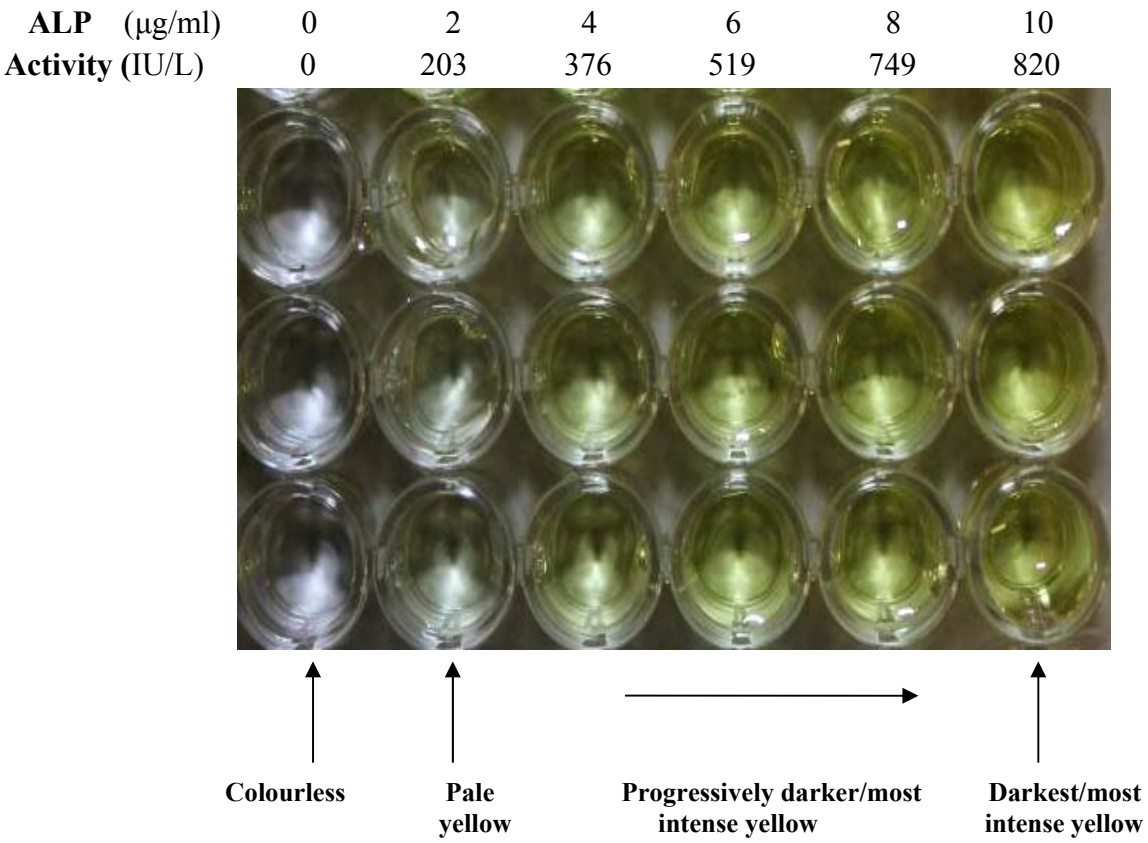

Figure 5.9a: Yellow colour intensities associated with enzyme activity of 10x diluted serum spiked with ALP. The experiments were carried out in triplicates and the yellow colour intensified with increase in enzyme activity.

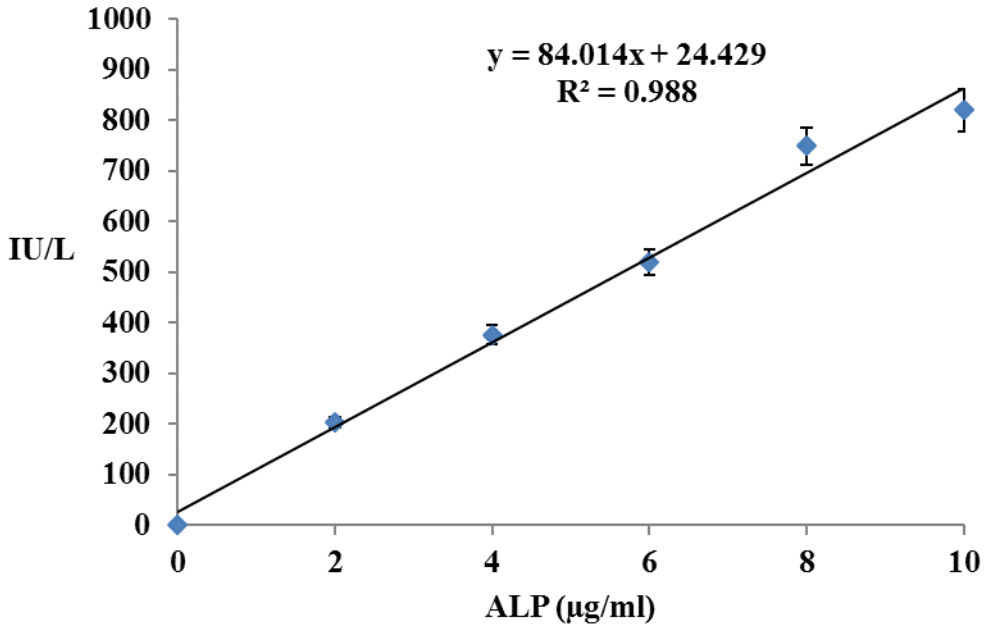

Figure 5.9b: Enzyme assaying standard curve of 10x diluted serum with ALP. Enzyme activity increased with increase in enzyme concentration. The experiments were carried out in triplicates and the error bars represent a 95 % confidence interval.

The fact that dilution of the serum enhanced the ability to detect ALP implied that removal of interferences can make assaying in biological matrices as sensitive as when a free enzyme is used. Furthermore, the results also showed that the probe may not only be limited to the use of plasma if serum was present. However, perhaps the device could be modified for serum samples by eliminating the haemoglobin filter since sample preparation of blood will not be necessary.

To summarise the findings, crude samples of serum should be diluted 10x since interferences absorb at the same wavelength as pNPL. We hypothesise that dilution of plasma obtained from filtered blood can also enhance the sensitivity of the colorimetric device since interferences will also be removed. Therefore, a buffer compartment should also be incorporated into the device to bring ALP to detectable levels. Lastly, serum and plasma could be used as sample matrices by the probe.

5.5 Nylon-para nitrophenyl phosphate nanofiber composites

The UV spectrum of nylon-pNPP composites in Fig. 5.10 showed an absorption band of 311 nm due to the charge transfer interactions. The solution remained colourless as observed in the picture insert and this indicated that the substrate did not decompose to pNPL which is yellow in colour.

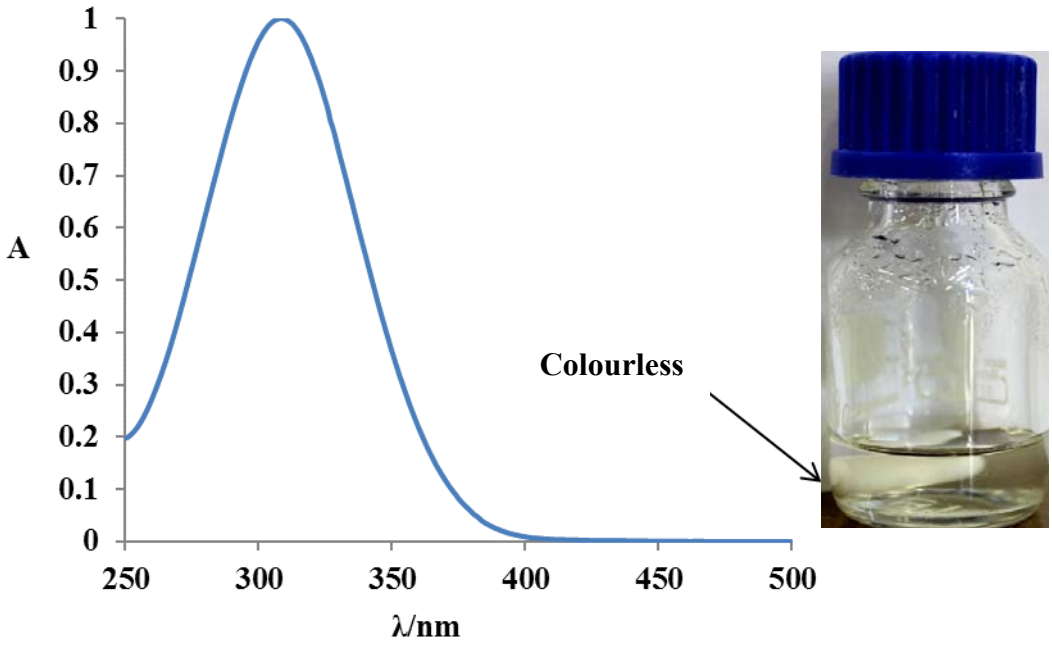

Figure 5.10: UV/Vis spectrum of nylon-pNPP polymer solution. The maximum absorbance was at 311 nm. The picture insert shows the colourless solution after blending for 12 h.

The substrate (pNPP) can become chemically unstable since the phosphate monoester bond is commonly prone to photolytic hydrolysis upon exposure to light which would have turned the solution yellow. Light energy hydrolyses the monoester bond by exciting the molecules to induce charge transfers which then cause a bathochromic shift to longer wavelengths of 405 nm and hence the yellow colour [123]. The shift is also a result of an increase in the bond order between nitrogen and oxygen and a decrease in the one between nitrogen and carbon. The transitions can therefore cause the bond to break hence it is important to cover the solution with aluminium foil during the stirring process.

Nylon was chosen because of its mechanical strength and ease of nanofibers fabrication. Further, the acids (acetic and formic) used for nylon dissolution also prevented hydrolysis of

the phosphate monoester bond as bases tend to also decompose pNPP. The decomposition can occur by hydroxides nucleophilically attacking the phosphoserly to elimination the phosphate. Then, the proton on the newly formed pNP can easily be removed by more hydroxides to form pNPL which is yellow in colour. Since pNPP did not decompose within the polymer after blending, the solution was therefore considered to be ready for electrospinning for synthesis of the nanofiber composites.

The synthesised nanofibers were characterized with SEM as can be seen in Fig. 5.11. They had a smooth morphology which was bead free while their average diameters were 20 nm.

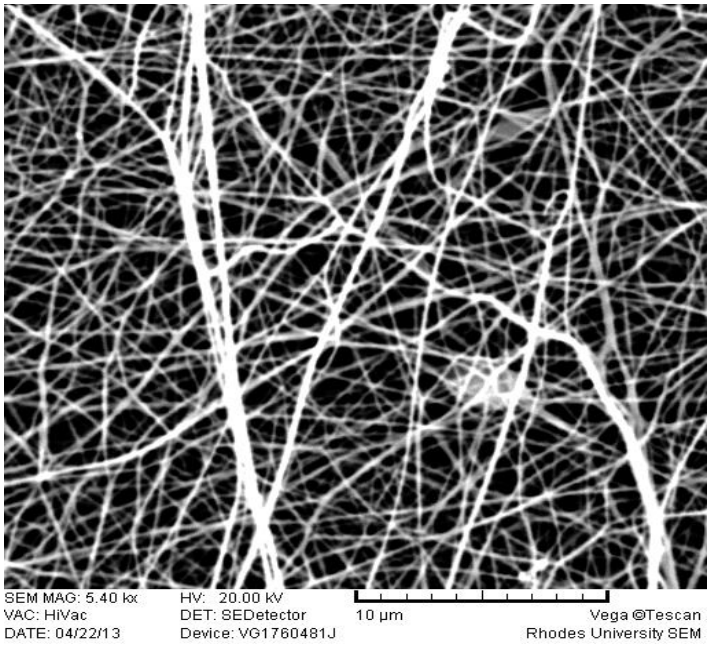

Figure 5.11: SEM image of nylon-pNPP nanofiber composites. Morphology was smooth and bead free and their average diameters were 20 nm.

The smooth morphology was due to the voltage overcoming the polymer surface tension as beads would have formed instead. Since the fibers were in the nanoscale, this showed that nanofibers were successfully synthesised. The small diameter also indicated that the fibers had a high surface area to volume ratio meaning they had a large platform to host the reaction between pNPP and ALP.

Interactions between pNPP and nylon nanofibers were non covalent (hydrogen bonding, ionic bonding and van der waals forces). The anticipated challenge with this type of immobilisation was leaching of the substrate since strong covalent attachment were not used.

This could be addressed by covalently attaching nylon to the ortho position of pNPP's benzene ring. However, when considering that only 20 µL of sample is required to assay, perhaps leaching might not be a serious challenge since it is not going to be applied as a dip stick which would profusely increase the level of leaching.

To confirm the presence of pNPP after electrospinning, further characterization was carried out using electron dispersive x-ray spectroscopy (EDS) (Fig. 5.12). The intension was to identify phosphorus and sodium as they were characteristic only to pNPP due to the fact that they were not present in either nylon or the solvents used.

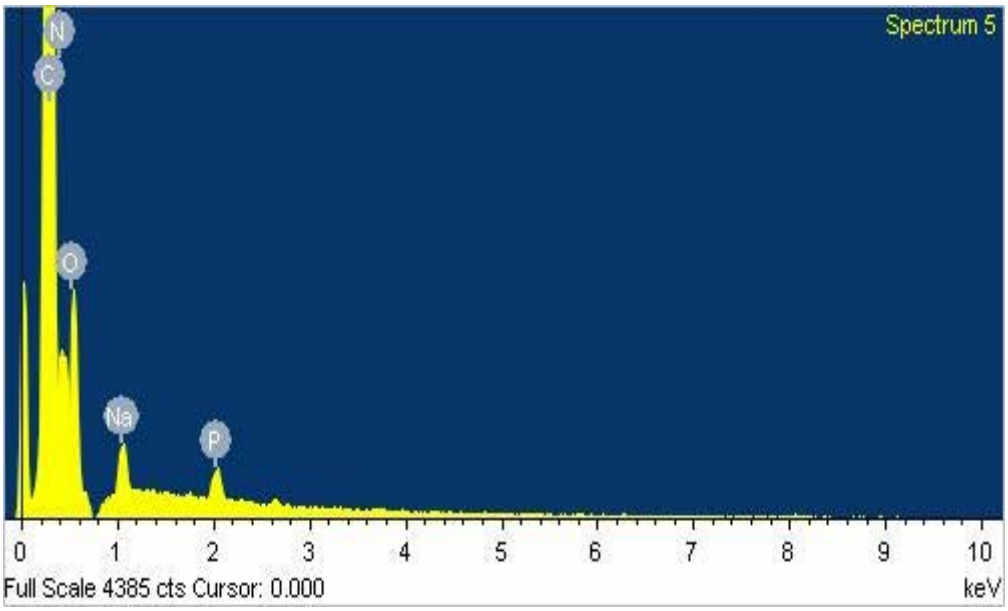

Figure 5.12: EDS spectra of nylon-pNPP nanofiber composites. Phosphorus and sodium elements were indicative of the presence of pNPP within the nanofiber after electrospinning.

It can be seen from the spectra that indeed these two elements were present indicating that pNPP was still within the nanofiber. Moreover, the fiber mats were also white after electrospinning as a yellow colour would have indicated breakage of the ester bond. The EDS findings were valuable in confirming that pNPP was still present within the nanofiber. In addition, the presence of pNPP further indicated that it did not evaporate with the solvents during the electrospinning process as this could have affected the accuracy of the assay.

In summation, pNPP in nylon polymer solution remained chemically stable during blending because it was not exposed to light while the acids for nylon dissolution also prevented hydrolysis of the phosphate monoester bond. The composites of nylon-pNPP nanofibers were successfully synthesised and pNPP was still present within the nanofiber even after electrospinning. The nanofibers were ready to be used as colorimetric probes for assaying ALP in the solid state.

5.6 Solid state assaying of Alkaline Phosphatase using nylon-para nitrophenyl phosphate nanofibers

Free ALP standards of 0, 2, 4, 6, 8 and 10 µg/ml which had the following respective activities; 0, 191, 376, 546, 700 and 858 IU/L, were assayed on the nylon-pNPP nanofibers as shown in Fig. 5.13. The control fiber mat (0 IU/L) remained white while there was a progressive increase in the yellow colour intensity with increase in enzyme activity. The distinct colours could clearly be observed within 5 min after which all the fibers developed the same colour intensity.

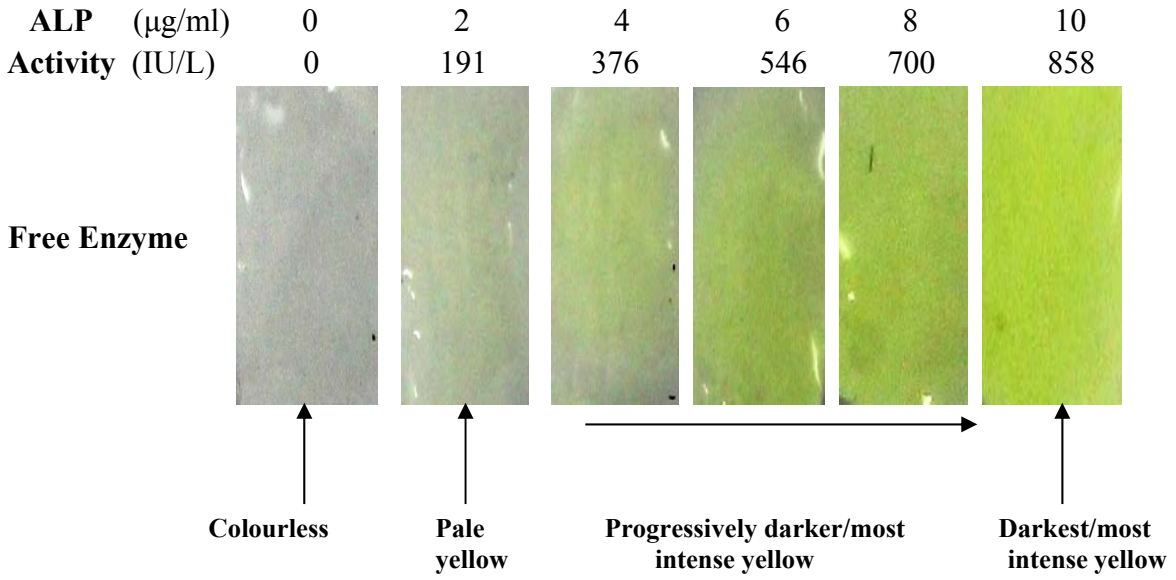

Figure 5.13: Solid state assaying of free ALP enzyme on nylon-pNPP nanofibers. There was a progressive increase in the yellow colour intensity with increase in enzyme activity.

The yellow colour observed after 5 min compared to 1 min in solution was due to the fact that the enzyme required more time to penetrate the porous fibers before catalysis could take place. This crucial observation indicated that 5 min was the optimal analysis time in order for

the probe to be accurate. The fibers all turned the same yellow colour intensity after 10 min because the reaction was not terminated as in solution. The enzyme continued to catalyse the reaction until the substrate was finished. The enzyme continued to catalyse the reaction until the substrate was finished. The reaction was not stopped because it was virtually impractical to do so but also to minimise the number of steps involved during diagnosis.

Similar to the experiments conducted in solution, the yellow colour was pale at enzyme activity between 0 and 191 IU/L which indicated that the colour would be invisible at 120 IU/L upper limit of normal. Therefore, with regards to diagnosis, the observation implied that the probe would be qualitative as it will only show a visual yellow colour above the normal level. However, for the probe to be semi-quantitative and accurate, it could perhaps be used together with a colour chart to distinguish the colours properly. Further, the highest 858 IU/L enzyme activity indicated that the nanofiber probe like in solution, could only detect up to 7.15x the upper limit of normal.

The anticipated challenge of leaching was encountered because a yellow colour could be observed on the liquid droplet instead of just on the nanofibers. This showed that pNPP leached into solution and that assaying was between the two phases. Nonetheless, in terms of the accuracy of the probe, leaching did not pose as a major drawback because the small sample of 20 μL was contained within the nanofiber. Therefore this indicated that all the assaying was still practically occurring on the nanofiber mat.

Assaying of 10x diluted serum spiked with ALP also demonstrated that there were no significant differences in the development of the yellow colours compared to the free ALP system (Fig. 5.14). The yellow colours also intensified with increase in enzyme activity and could also be distinctly identified after 5 min. The serum probe could only detect up to 6.84x the normal limit which is slightly lower than 7.15x observed for the free ALP system although not significant. These findings as in solution assaying implied that diluting the biological samples of serum or plasma would be necessary for the colorimetric device to enhance sensitivity. They also showed that dilution would make detection of ALP in biological samples as accurate as when a free enzyme system was assayed. However the fibers were still leaching as was also observed in fibers assayed with free ALP.

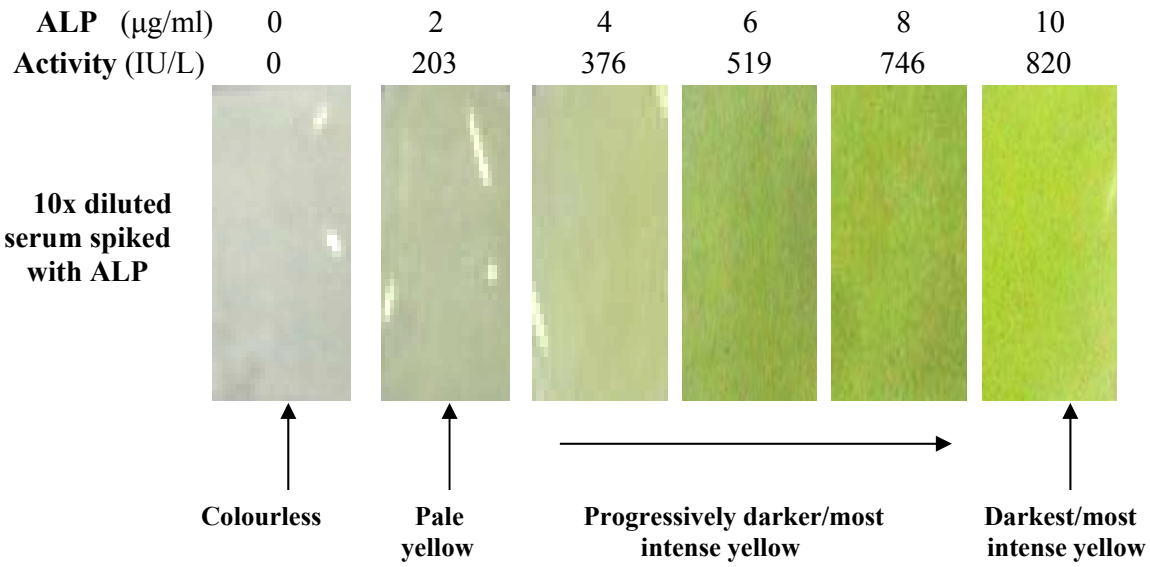

Figure 5.14: Solid state assaying of 10x diluted serum spiked with ALP on nylon-pNPP nanofibers. There was a progressive increase in the yellow colour intensity with increase in enzyme activity.

To sum up the results, there was a progressive intensity increase of the yellow colour on the nylon-pNPP nanofibers mats as enzyme activity of ALP increased. The results also indicated that the colour would be invisible at the upper limit of normal (120 IU/L) which is a desirable feature for the probe to possess. Further, the analysis time for the probe should be 5 min since the distinct yellow colours could only be observed within that time limit. However, there was no significant difference in the behaviour of the probe when free ALP or 10x diluted serum spiked with ALP were assayed. Leaching was also observed during the assaying even though it did not pose a major challenge since the sample droplet was contained on the nanofiber during assaying.

5.7 Leaching of para nitrophenyl phosphate from the electrospun nanofibers layer

Since leaching of pNPP into solution was inevitable as already observed during the solid state assaying, it was therefore important to address it. Although the concentration of pNPP that leached into solution could not be quantified, the rate would still be a good indicator of the extent of leaching. The results are shown in Fig. 5.15 and it can be seen that the rate of pNPP leaching increased with time. There was a linear increase until 1.25 min after which from 1.5 to 2.5 min it reached a plateau. This indicated that the rate was extremely fast also when considering the fact that it was already 1.37×10^{-3} A/min^{-1} after only the first interval.

Absorbance was monitored at 305 nm because the UV/Vis spectrum (Fig. 5.1b) showed that maximum absorbance of pNPP was at that wavelength.

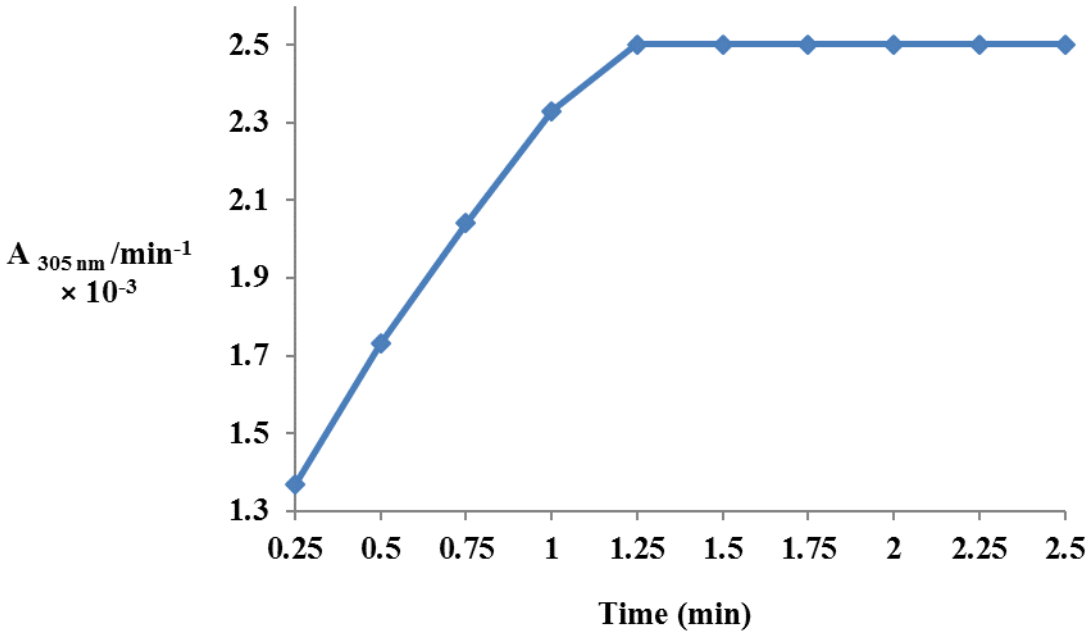

Figure 5.15: The rate of pNPP leaching into solution from the nanofiber layer. Leaching increased linearly until 1.25 min after which it reached a plateau.

The graph confirmed that indeed leaching of pNPP would have to be addressed to ensure catalysis only occurred on the surface of the nanofiber. Moreover, the results also indicated that the probe would not be suitable as a dip stick since all the pNPP would leach into solution. Furthermore, even though leaching was established to not be a major challenge due to the sample droplet being contained on the nanofiber, it would still be ideal to minimise it as much as possible by covalent bonds. Nylon could be attached to the ortho position of pNPP's benzene ring via synthesis methods such as lithiation.

Therefore, in summary, the graph indicated that the rate of pNPP leaching from the nanofiber layer was extremely high and that it would have to be addressed by covalently attaching nylon to the benzene ring of pNPP for future work.

5.8 Effect of heat on the chemical stability of nylon-para nitrophenyl phosphate nanofiber composites

The preliminary data on the effect of heat treatment on nylon-pNPP nanofiber composites is presented in Fig. 5.16a (40 ºC) and 5.17a (80 ºC). After the nanofibers were heated for 12 h at these two temperatures, they were used to assay free ALP (10 µg/ml standard) to determine whether the yellow colours from pNPL would still be observed. For heat treatment at 40 ºC, the control mat remained white while the assay mat turned yellow. The morphology (Fig. 5.16b) of the fibers also remained unchanged after treatment but the pores seemed to have decreased given that both were viewed at the same magnification of 20 µm.

Control mat (0 µg/ml)

Mat assayed with 10 µg/ml free ALP

Figure 5.16a: ALP assaying on nylon-pNPP nanofiber mats after 40 ºC heat treatment. The mats were white after treatment. The control mat remained white while the mat assayed with 10 µg/ml free ALP turned yellow.

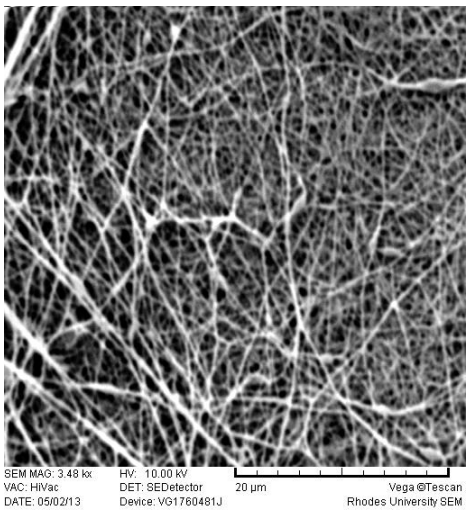

Before heat treatment

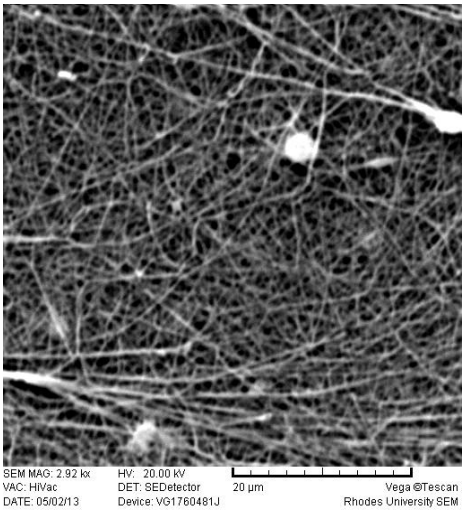

After 40 ºC heat treatment

Figure 5.16b: SEM images comparing nylon-pNPP nanofiber mats before and after 40 ºC heat treatment. The morphology of the fibers remained unchanged while the pores seemed to have decreased considering that both were viewed at the same magnification of 20 µm.

Heat treatment at 80 ºC however turned the mats yellow indicating that the high temperature hydrolysed the phosphate monoester bond (Fig. 5.17a). Hydrolysis of the substrate meant the mats could not be used for ALP assaying as can be observed in figure that both mats were yellow. The SEM images in Fig. 5.17b also showed that the morphology remained unchanged after treatment although the pores also seemed to have significantly decreased.

Control mat
(0 µg/ml)

Mat assayed with
10 µg/ml free ALP

Figure 5.17a: ALP assaying on nylon-pNPP nanofiber mats after 80 ºC heat treatment. The mat turned yellow after treatment meaning the 10 µg/ml ALP standard was not responsible for the yellow colour observed.

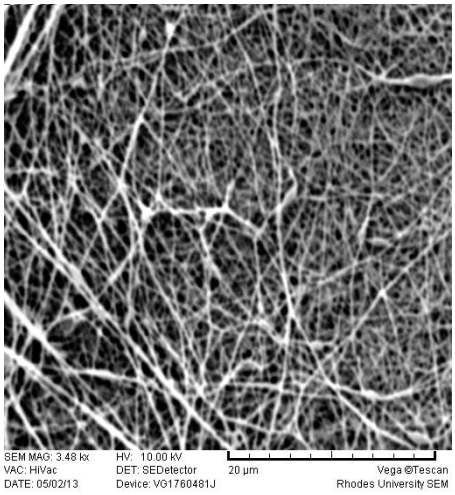

Before heat treatment

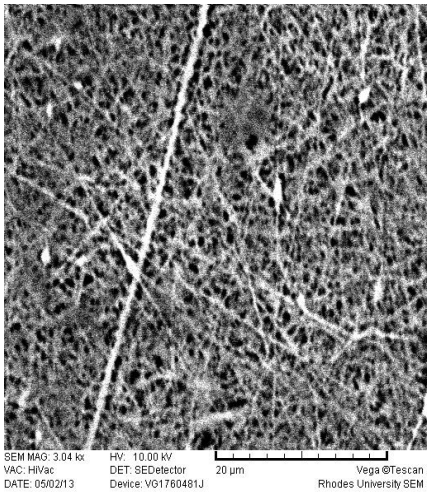

After 80 ºC heat treatment

Figure 5.17b: SEM images comparing nylon-pNPP nanofiber mats before and after 80 ºC heat treatment. The morphology of the fibers remained unchanged while the pores seemed to have decreased considering that both were viewed at the same magnification of 20 µm.

The pores decreased at both temperatures because heat can evaporate moisture responsible for swelling the fibers and creating the pores. Heat causes the fibers to contract lengthwise and diametrically therefore causing them to shrink and curl up. Normally fibers are porous because the moisture tends to expand them. Hydrolysis of pNPP after 80 ºC heat treatment on the other hand was caused by thermal effects. The heat or bond energy was sufficiently high enough to break the phosphate monoester bond as opposed to the energy at 40 ºC. These preliminary results suggested that pNPP was not chemically stable beyond temperatures of 40 ºC. However, a systematic study of the effect of temperature on the chemical stability of pNPP must be carried out in order for conclusive results to be obtained.

Nonetheless, chemical stability results of pNPP were useful in assessing the practical applicability of the probe in telemedicine. The fact that pNPP was chemically stable at 40 ºC within the fibers showed that the probe could be suitable for use in hot climate areas such Sub-Saharan Africa where telemedicine is commonly practiced in rural and resource poor settings. These experiments also indicated that pNPP would not decompose before the probe reached its intended destination. Furthermore, the chemically stability of pNPP at 40 ºC also indicated that the probe would not have to be stored at pNPP's storage temperature of 4 ºC since most resource poor areas do not have refrigerators. However, to confirm these conclusions, the shelf life of the probe would have to be studied.

To summarise, the preliminary results indicated that pNPP was chemically stable at temperatures below 40 ºC which implied that the probe could be practically applicable in hot climate areas where telemedicine is normally practiced. Nevertheless, even though pNPP decomposed at 80 ºC, further work must be carried out to study the effect of temperature on the chemical stability of the substrate.

Chapter 6

6. Conclusion and Future work

6.1 Conclusion

The findings from the experimental studies conducted in this thesis demonstrated that pNPP, pNP and pNPL behaved as expected in their respective pH mediums of biological (7.4), acidic (pH 2) and basic (pH 9). The pNPL chromophore exhibited a strong molar extinction coefficient (ε) of 18,458 M^{-1} cm^{-1} which indicated that it was suitable to be used in ALP kinetics and assaying studies. Kinetic models using the more accurate LB plot showed that ALP had V_{max}, K_m and an excess substrate of 5.5×10^{-3} μmol/min^{-1}, 0.025 mM and 0.25 mM respectively. Furthermore, ALP assaying in free systems and serum solution samples was successfully carried out in solution. Synthesis of nylon-pNPP electrospun nanofibers was also successful as they were used as colorimetric probes. The yellow colour of the probes intensified with increase in enzyme activity. In addition, analysis time of the probes was determined to be 5 min as distinct colours could only be observed within that time. The rate of leaching was extremely fast since pNPP was not covalently attached to nylon. Finally, temperatures below 40 ºC were determined to maintain the chemical stability of pNPP within the fibers. Therefore, nylon-pNPP nanofibers were determined to be suitable for the development of the proposed colorimetric diagnostic device capable of detecting ALP for point of care liver toxicity diagnosis.

6.2 Future work

It is recommended that further work be carried out using plasma obtained from filtration of a diseased patient's blood as this would determine the applicability of this novel probe in real samples. Moreover, the effect of temperature on the chemical stability of pNPP should also be studied as well as the probe's shelf life over time. These experiments will be highly valuable in evaluating the practical applicability of the probe in resource poor and rural areas which practice telemedicine.

References

[1] Xu, J. J., Diaz, D., O'Brien, P. J., 2004. *Chem. Biol. Interact*., 150: 115-128.

[2] Ozer, J., Ratner, M., Shaw, M., Bailey, W., Schomaker, S., 2008. *Toxicology*., 245: 194-205.

[3] Jones, M., Nunez, M., 2012. *Semin. Liver Dis*., 32: 167-176.

[4] Bonacini, M., 2004. *Clin. Infect. Dis*., 38: 104-108.

[5] Calmy, A., Hirschel, B., Cooper, D. A., Carr, A., 2009. *Antivir. Ther*., 14: 165-179.

[6] Carr, A., 2003. *Nat. Rev. Drug Discov*., 2: 624-634.

[7] Bianchi, A., Giachetti, E., Vanni, P., 1994. *J. Biochem. Biophys. Methods*., 28: 35-41.

[8] Gong, H., Little, G., Cradduck, M., Draney, D. R., Padhye, N., Olive, D. M., 2011. *Talanta*., 84: 941-946.

[9] Lindor, K. D., Talwalker, J. A., 2008. *Cholestatic Liver Disease*., 1st ed. Humana Press. United States of America. 2.

[10] Mayo Medical Laboratories., Alkaline Phosphatase, Total and Isoenzymes, Serum., Mayomedicallaboratories.com. 24th June 2013. Available at: http://www.mayomedicallaboratories. com/test-catalog/Clinical+ and +Interpretive/89503.

[11] Latner, A. L., Parson, M. E., Skillen, A.W., 1970. *Biochem. J*., 118: 299-302.

[12] Bitesizebio., Colorimetric Assay., Bitesizebio.com. 20th April 2013. Available at: http://bitesizebio.com/articles/ask-a-chemist-how-colorimetric-assays-work.

[13] Bioscience., Protein Assay Handbook for Selection Guide., Gbioscience.com. 20th April. Available at: http:// info.gbiosciences.com/complete-protein-assay-guide/.

[14] World Health Organisation., 1998. *A Health Telematics Policy in Support of WHO's Health-For-All Strategy for Global Health Development: Report of the WHO Group Consultation on Health Telematics*., World Health Organization.11-16.

[15] Wu, L., Yuan, X., Sheng, J., 2004. *J. Mater. Sci*., 250: 167-173.

[16] Doshi, J., Reneker, D. H., 1995. *J. Electrostat*., 35: 151-160.

[17] Raghavan, P., Lim, D., Ahn, J., Nah, C., Sherrington, D. C., Ryu, H., Ahn, H., 2012. *React. Funct. Polym*., 72: 915-930.

[18] Sill, T. J., Recum, H., 2008. *Biomaterials*., 29: 1989-2006.

[19] Vella, S. J., Beattie, P., Cademartiri, R., Laromaine, A., Martinez, A. W., Phillips, S. T., Mirica, K. A., Whitesides, G. M., 2012. *Anal. Chem*., 84: 2883-2891.

[20] Roupon, R., Chazouillkes, O., Roupon, R. E., 2000. *J. Hepatol*., 35: 129-140.

[21] Halilbasic, E., Baghdasaryan, A., Trauner, M., 2013. *Clin. Liver Dis*., 17: 161-189.

[22] Schlaeger, R., Haux, P., Kattermann, R., 1982. *Enzyme*., 28: 3-13.

[23] European Association for the Study of the Liver., 2009. *J. Hepatol*., 51: 237-267.

[24] Medical University of South Africa., Serum Alkaline Phosphatase Measurement. 18th October 2013. Muschealth.com. Available at: http://www.muschealth.com/lab/content. aspx?id= 150031.

[25] Shukla, A. N., 2009. *Chemistry of Enzymes*., 1st ed. Discovery Publishing House. India. 35.

[26] Copeland, R. A., 2005. *Evaluation of Enzyme Inhibitors in Drug Discovery*., 1st ed. John Wiley & Sons. United States of America. 88-89.

[27] Prasad, N. K., 2011. *Enzyme Technology*., 1st ed. PHI Learning Private. India. 212.

[28] Hehir, M. J., Murphy, J. E., Kantrowitz, E. R., 2000. *J. Mol. Biol*., 304: 645-656.

[29] Yoshuzumi, F. Y., Coleman, J. E., 1974. *Arch. Biochem. Biophys*., 160: 255-268.

[30] Garattini, E., Hua, J. C., Pan, Y. C., Udenfriend, S., 1986. *Arch. Biochem. Biophys*., 245: 331-337.

[31] Kim, E. E., Wyckoff, H. W., 1991. *J. Mol. Biol*., 218: 449-464.

[32] Zalatan, J. G., 2006. *Biochemistry*., 45: 9788-9808.

[33] Zalatan, J. G., Fenn, T. D., Herschlag, D., 2009. *J. Mol. Biol*., 384: 1174-1189.

[34] Conyers, R. A. J., Birkett, D.J., Neale, F.C., Posen, S., 1967. *Biochim. Biophys. Acta*., 139: 363-371.

[35] Koay, E. S. C., Walmsely, N., 1996. *A Primer and Chemical Pathology*., 1st ed. World Scientific Publishing. 157.

[36] Guguen-Guillouzo, C., 2002. *Culture of Epithelial Cells*., 2nd ed. Wiley-Liss. France. 239.

[37] Down, J. E., Riggs, D. S., 1965. *J. Bio. Chem*., 240: 863-869.

[38] Wilson, K., Walker, J., 2005. *Principles and Techniques of Biochemistry and Molecular Biology*., 6th ed. Cambridge University Press. United States of America. 557-578.

[39] Purich, D. L., 2009. *Contemporary Enzyme Kinetics and Mechanism: Reliable Lab Solutions*., 3rd ed. Elservier. United Kingdom. 1-5.

[40] Whitehurst, R. J., Van Oort, M., 2010. *Enzymes in Food Technology*., 2nd ed. Blackwell Publishing. United States of America. 1-16.

[41] Campbell, K. M., Farrell, S. O., 2012. *Biochemistry*., 7th ed. Brooks. United States of America. 165.

[42] Dept of Washington., Michaelis-Menten Kinetics & Briggs-Haldane Kinetics., Dept of Washington.edu. 8th September 2013. Available at: http://depts.washington.edu/wmatkins/kinetics/michaelis-menten.html.

[43] The Medical Biochemistry., Introduction to Enzymes., The Medical Biochemistry Page.org. 8th September 2013. Available at: http://themedicalbiochemistrypage.org/enzyme-kinetics.php.

[44] Stoker, H. S., 2010. *General, Organic and Biological Chemistry*., 5th ed. Brooks/Cole. United States of America. 705-709.

[45] Campbell, M. K., Farrell, S. O., 2007. *Biochemistry*., 6th ed. Brooks/Cole. United States of America. 160.

[46] Thompson, R. Q., Barone, G. C., Halsall, H. B., Heineman, W. R., 1991. *Anal. Biochem*., 192: 90-95.

[47] Bowers, G. N., McComb, R. B., Christensen, R. C., Schaffer, R., 1980. *Clin. Chem*., 26: 724-729.

[48] Moore, J. W., Stanitski, C. L., Jurs, P. C., 2008. *Chemistry: The Molecular Science*., 3rd ed. Brooks/Cole. United States of America. 406.

[49] Ucdavis., Ultraviolet and Visible Spectroscopy., Chemiwiki.ucdavis.edu. 18th October 2013. Available at: http://chemwiki.ucdavis.edu/Organic_Chemistry/Organic_Chemistry_With_a_ Biological_Emphasis/Chapter__4%3A_Structure_Determination_ I/Section_ 4.3%3A_Ultraviolet_and_visible_spectroscopy.

[50] MacKintosh, C., 1993. *Protein Phosphorylation: A practical Approach*., 1st ed. IRL Press. United States of America. 221.

[51] Zhuo, S., Clemens, J. C., Hakes, D. J., Barfold, D., Dixon, J. E., 1993. *J. Biol. Chem*., 268: 17754-17761.

[52] Zhang, Z. Y., Clemens, J. C., Schubert, H. L., Stuckey, J. A., Fischer, M.W., Hume, D. M., Saper, M. A., Dixon, J. E., 1992. *J. Biol. Chem*., 267: 23759-23766.

[53] Pot, D. A., Woodford, T. A., Remboutsika, E., Haun, R. S., Dixon, J. E., 1991. *J. Biol. Chem*., 266: 19688-19696.

[54] Marie-Christine, D., Didier, Astruc., 2004. *Chem. Rev*., 104: 293- 346.

[55] Chen, Y. M., Yu, C. J., Cheng, T. L., Tseng, W. L., 2008. *Langmuir*., 24: 3654-3660.

[56] Wei, H., Chen, C., Han, B., Wang, E., 2008. *Anal. Chem*., 80: 7051-7055.

[57] Sepulveda, B., Angelome, P.C., Lechuga, L.M., Liz-Marzan, L.M., 2009. *Nanotoday*., 4: 224-251

[58] Toma, H. E., Zamarion, V. M., Toma, S. H., Araki, K., 2010. *J. Braz. Chem. Soc*., 21: 1158-1176.

[59] Liu, R., Liew, R., Zhou, J., Xing, B., 2007. *Angew. Chem*. Int. Ed., 46: 8799-8803.

[60] Liu, D. B., Qu, W. S., Chen, W. W., Zhang, W., Wang, Z., Jiang, X. Y., 2010. *Anal. Chem*., 82: 9606-9610.

[61] Choi, Y., Ho, N. H., Tung, C. H., 2007. *Angew. Chem. Int. ed*., 46: 707-709.

[62] Wu, Z., Zhang, B., Yan, B., 2009. *Int. J. Mol. Sci*., 10: 4198-4209.

[63] Lakowicz, J. R., 2010. *Principles of Fluorescence Spectroscopy*., 3rd ed. Springer. United States of America. 5.

[64] Sykes, A. G., 1990. *Advances in Inorganic Chemistry*., 1st ed. Academic Press. United Kingdom. 387.

[65] Malapit, C. A., 2010. *Synthesis of Fluorescein, a Fluorescent Dye*., 1st ed. Ateneo de Manila University. Phillipines. 1-2.

[66] Montalibet, J., Skorey, K. I., Kennedy, B. P., 2005. *Methods*., 35: 2-8.

[67] Wang, Q., Scheigetz, J., Gilbert, M., Snider, J., Ramachandran, C., 1999. *Biochim. Biophys. Acta*., 1431: 14-23.

[68] Merts, D., 2011. *J. Mater. Chem*., 21: 8324-8325.

[69] Magde, D., Wong, R., Seybold, P.G., 2002. *J. Photochem. Photobiol*., 75: 327-334.

[70] Sjoback, R., Nygren, J., Kibista, M., 1995. *Spectrochem. Acta. Part A*., 51: 7-21.

[71] Liu, M., Lin, Z., Lin, J., 2010. *Anal. Chim. Acta*., 670: 1-10.

[72] Calokerinos, C., Deftereos, N. T., Baeyens, W. R. G., 1995. *J. Pharm. Biomed. Anal.*, 13: 1063-1071.

[73] Baeyens, W. R. G., Schulman, S.G., Calokerinos, A. C., Zhao, Y., Campana Garcia, A. M., Nakashima, K., Keukeleire, D. De., 1998. *J. Pharm. Biomed. Anal.*, 17: 941-953.

[74] Arakawa, H., Shiokama, M., Imamura, O., Aeda, M., 2003. *Anal. Biochem*., 314: 206-211.

[75] Kricka, L. J., 2003. *Anan. Chim. Acta*., 500: 279-286.

[76] Life Technology., 2013. *The Molecular Probe Handbook*., 1st ed. Life Technology. United States of America. 9.

[77] Ximenes, V. F., Campa, A., Baader, W.J., Catalani, L.H., 1999. *Anal. Chim. Acta*., 402: 99-104.

[78] Degraff, B. A., Horner, D. A., 1996. *J. Chem. Edu*., 73: 279-285.

[79] Zoski, G. C., 2007. *Handbook of Electrochemistry*., 1st ed. Elsevier. United Kingdom. 3.

[80] Newman, J., Thomas-Alyea, K. E., 2004. *Electrochemical Systems*., 3rd ed. John Wiley & Sons. United States of America. 2.

[81] Tyagi, P., 2006. *Electrochemistry*., 1st ed. Discovery Publishing House. India. 1.

[82] Skoog, D. A., West, D.M., Holler, F.M., Crouch, S. R., 2004. *Fundamentals of Analytical Chemistry*., 8th ed. Brooks/Cole. United States of America. 490.

[83] Iqbal-Asef, M., Gupta, S. G., Hussaini, S. S., 2012. *Adv. Bio. Res*., 3: 158-163.

[84] Ronkainen, N. J., Halsall, H. B., Heinman, W. R., 2010. *Chem. Soc. Rev*., 39: 1747-1763.

[85] Ito, S., Yamazaki, S., Kano, K., Ikeda, T., 2000. *Anal. Chim. Acta*., 424: 57-63.

[86] Ruan, C., Li, Y., 2001. *Talanta.*, 54: 1095-1103.

[87] Juttner, K. J., 2007. *Technical Scale of Electrochemistry*., 1st ed. Wiley. United States of America. 3.

[88] Kim, H., Kwak, J., 2005. *J. Electroanal. Chem*., 577: 243-246.

[89] Wild, D. G., 2013. *The Immunoassay Handbook*., 4th ed. Elservier. United Kingdom. 7.

[90] Dyakov, Y., Dzhavakhiya, V., Korpela, T., 2007. *Comprehensive and Molecular Phytopathology*., 1st ed. Elservier. United Kingdom. 77.

[91] Pei, X., Zhang, B., Tang, J., Liu, B., Lai, W., Tang, D., 2013. *Anal. Chim. Acta*., 758: 1-18.

[92] Rongen, A. H., Bult, A., Van-Bennekom, W. P., 1997. *J. Immunol. Methods*., 204: 105-133.

[93] Butler, J., 2000. *J. Immunoassay*., 21: 165-209.

[94] Funk, C. J., 2001. *Arch. Insect. Biochem. Physiol*., 46: 165-174.

[95] Jekely, G., Arendt, D., 2007. *Biotech*., 42: 751-755.

[96] Activemotif., Function ELISA Signalling Protein ELISAs., Activemotif.com. 20th September 2013. Available at: http://www.activemotif.com/catalog/162/functionelisa-signaling-protein-elisas.

[97] Basso, A., Martin, L. D., Ebert, C., Linda, P., Gardossi, L., Rein V. Ulijn, R.V., Flitsch, S.L., 2003. *Tetrahedron Lett*., 44: 6083-6085.

[98] Deitzel, J. M., 2001. *Polymer*., 42: 261-264.

[99] Dalton, P. D., 2007. *Polymer*., 48: 6823-6833.

[100] Chronokis, I. S., 2005. *J. Mater. Process Tech*., 167: 283-293.

[101] Reneker, D. H., Alexander, L., Hao, F., Koombhongse, S., 2000. *J. Appl. Phys*., 87: 4531-4547.

[102] Dalton, P. D., Lleixa Calvet, J., Mourran, A., Klee, D., Möller, M., 2006. *Biotechnol. J*., 1: 998-1006.

[103] Shin, M. Y., Hohman, M. M., Brenner, M., Ruteldge, G. C., 2001. *Polymer*., 42: 9955-9967.

[104] Lin, T., Wang, H., Wang, X., 2005. *Adv. Mater*., 17: 2699-2703.

[105] Qin, X. H.,Wan, Y. Q., He, J. H., Zhang, J., Yu, J. Y., Wang, S. Y., 2004. *Polymer*., 45: 6409-6413.

[106] Bhardwaj, N., Kundu, S. C., 2010. *Biotech. Adv*., 28: 325-347.

[107] Taylor, G., 1969. *Proc. R. Soc. Lond. A*., 313: 453-475.

[108] Martin, C. R., 1996. *Chem. Mater*., 8: 1739-1746.

[109] Ma, P. X., Zhang, R., 1999. *J. Biomed. Mat. Res*., 46: 60-72.

[110] Chigome, S., Torto, N., 2011. *Anal. Chim. Acta*., 706: 25-36.

[111] Yuan, X., Zhang, Y., Dong, C., Sheng, L., 2004. *Polym. Int*., 53: 1704-1710.

[112] Clugstron, M., Rosalind, F., 2000. *Advanced Chemistry*.,1st ed. Oxford University Press. United Kingdom. 104-105.

[113] Jeon, H., Lee, J., Kim, M. H., Yoon, J., 2012. *Macromol. Rapid Commun*., 33: 972-976.

[114] Yoon, B., Lee, S., Kim, J. M., 2009. *Chem. Soc. Rev*., 38: 1958-1968.

[115] Yoon, S. K., Kim, J. M., 2007. *J. Am. Chem. Soc*., 129: 3038-3039.

[116] Dubitsky, A., Fomovska, G., Use of Vivid Plasma Separation Membrane For Sensitive Detection of Troponin in Whole Blood Samples., Pall.com. 3rd March 2014. Available at: http://www.pall.com/pdfs/OEM-Materials-and-Devices/10-3554 Oak RidgeConfPSTR.pdf.

[117] Naeem, A., Khan, I. M., Ahmad, A., 2011. *J. Phys. Chem*., 85: 1840-1843.

[118] Hengge, A. C., Cleland, W.W., 1990. *J. Am. Chem. Soc*., 112: 7421-7422.

[119] Reusch, W., Spectroscopy., Chemistry.msu.edu. 16th May 2013. Available at: http://www2. chemistry.msu.edu/Faculty/reusch/VirtTxtJml/Spectrpy/UV-Vis/spectrum.htm.

[120] Bansal, R. K., 2003. *A Textbook of Organic Chemistry*., 4th ed. New Age International Publishers. India. 135.

[121] Voet, D., Voet, J. G., 2004. *Biochemistry*., 3rd ed. Wiley. United States of America. 479.

[122] Wilson, K., Walker, J., 2000. *Principles and Techniques of Biochemistry and Molecular Biology*., 5th ed. Cambridge University Press. United Kingdom. 679.

[123] Dennis, P. B., Walker, A. Y., Dickerson, M. B., Kaplan, D. L., Naik, R. R., 2012. *Biomacromolecules*., 13: 2037-2045.